Crop and Environment 5 (2026) 100111

Contents lists available at ScienceDirect

Crop and Environment

journal homepage: www.journals.elsevier.com/crop-and-environment

Original Article

Moderate late sowing balances wheat yield and dough quality by regulating temperature-mediated nitrogen accumulation and translocation

Yakun Li[a], Xidan Cao[a], Jingyi Feng[a], Huihui Hu[a], Yi Liu[a], Vinay Nangia[c], Yang Liu[a,b,*]

[a] College of Agronomy, Northwest A&F University, Yangling, Shaanxi 712100, China
[b] State Key Laboratory for Crop Stress Resistance and High-Efficiency Production, Northwest A&F University, Yangling, Shaanxi 712100, China
[c] International Center for Agricultural Research in the Dry Areas, Rabat 999055, Morocco

ARTICLE INFO

Keywords:
Dough microstructure
Dough quality
Nitrogen accumulation
Sowing date
Temperature conditions
Wheat

ABSTRACT

Although numerous studies have reported the effects of late sowing on wheat yield, its impact on the microstructure and processing quality of wheat dough remains unclear. This study aimed to investigate how late sowing influenced wheat quality, with a focus on both the general characteristics and fine structure of dough. A two-factor split-plot field experiment was conducted during the 2020–2022 growing seasons. Sowing date was assigned as the main plot, including four treatments: T1 (October 8), T2 (October 20), T3 (November 1), and T4 (November 13). The subplot was wheat variety, comprising two strong-gluten varieties and two medium-gluten varieties. Results indicated that appropriately late sowing altered the source-sink ratio, enhanced nitrogen uptake and accumulation in wheat plants, and significantly increased grain protein content and protein yield. At T3, protein content increased by 1.71%–27.22%, and protein yield increased by 3.32%–15.42% compared with other sowing dates. Furthermore, late sowing improved the microstructure of the dough and enhanced the processing quality of the flour. The Mantel test and structural equation modeling revealed that moderate delay in sowing improved thermal conditions from wintering to flowering stage, which promoted nitrogen accumulation and translocation within the plants and increased the contents of protein and glutenin subunits in the grain. These changes ultimately optimized the dough microstructure and improved the processing quality of wheat. With the delay of sowing date, the grain yield of four wheat varieties peaked at T2 in both 2020-2021 and 2021-2022 growing seasons. Our study provides a theoretical reference for how sowing date affects wheat yield and quality.

1. Introduction

Wheat is a crucial staple crop, providing essential protein and starch and contributing approximately 20% of the global energy intake (Ottaiano et al., 2022). As the global population grows and living standards improve, the demand for high-quality wheat is increasing. Consequently, research on the selection and breeding of superior wheat varieties and the enhancement of wheat quality through cultivation practices has gained prominence (Liu, 2023; Singh et al., 2021; Tao et al., 2018; Zheng et al., 2021). The sowing date is a critical agronomic factor in wheat production, significantly influencing wheat growth and development (Ferrise et al., 2010; Ma et al., 2018; Shah et al., 2020). Recent global temperature increases and frequent warm winters have led to a common phenomenon of late sowing in wheat production. Climate change has resulted in more frequent extreme weather events (Wijerathna-Yapa and Pathirana, 2022). For instance, in wheat-maize rotation areas, continuous rainfall during maize harvesting and wheat sowing, combined with extensive field operations such as harvesting, plowing, fertilizing, and planting, has further delayed wheat sowing (Shah et al., 2020; Zheng et al., 2012). A moderate delay in sowing can enhance root activity, leaf photosynthetic capacity, and the resistance of winter wheat to failure, while maintaining seed yield and nitrogen use efficiency (Dai et al., 2017). However, late sowing also reduces light and temperature availability before winter, accelerates the reproductive process, and decreases the ratio of vegetative to reproductive growth phases. This results in fewer tillers and less preflowering dry matter

---

* Corresponding author.
E-mail address: yangl@nwafu.edu.cn (Y. Liu).

https://doi.org/10.1016/j.crope.2025.10.001
Received 8 July 2025; Received in revised form 9 October 2025; Accepted 12 October 2025

accumulation, ultimately reducing wheat yield (Liu et al., 2023; Zhang et al., 2022a). These findings indicate that the sowing date significantly impacts wheat growth and yield.

Protein, constituting 10–18% of wheat flour, is crucial for determining the rheological properties of dough and the overall quality of the flour. Late sowing increases the protein, glutelin, and high molecular-weight glutenin subunit (HMW-GSs) contents in wheat grains, enhances dough stability, alters dough rheological properties, and improves wheat processing quality (Li et al., 2013; Mahdavi et al., 2022; Ottaiano et al., 2022). However, some studies indicated that late sowing could either significantly decrease processing quality despite increasing protein content or had no significant effect on either (Chu et al., 2023; Dong et al., 2022). Most studies have linked late sowing to increased protein deposition due to high temperature during the grain-filling stage (Mirosavljević et al., 2024; Singh et al., 2021; Sissons et al., 2018). However, changes in sowing dates lead to alterations in wheat phenology (Ma et al., 2018; Rossini et al., 2024; Shah et al., 2020), resulting in different temperature conditions during various growth stages, not just during the grain-filling period. The vegetative growth stage is the peak period for nitrogen absorption and accumulation in wheat, and temperature changes during this stage affect nitrogen accumulation in plants before flowering (Cai et al., 2016; Kong et al., 2023). The protein content in wheat is primarily determined by the translocation of nitrogen from vegetative organs to the grains after flowering (Austin et al., 1977; Ferrise et al., 2010). Nevertheless, only a few studies have examined the impact of temperature changes throughout the entire growth cycle under different sowing dates on nitrogen accumulation and remobilization in plants and their relationship with protein content (Dong et al., 2022; Ferrise et al., 2010). Therefore, it is essential to analyze the effects of temperature variations during different growth stages caused by changes in sowing dates on nitrogen absorption and remobilization in wheat plants throughout the entire growth cycle in order to understand the mechanisms underlying the response of wheat grain yield and quality to sowing dates.

Previous research has focused primarily on the impact of sowing date on wheat grain protein content. In addition to protein content, gluten secondary structure, dough microstructure, HMW-GSs, and low molecular weight glutenin subunits (LMW-GSs) likewise have significant effects on wheat quality and end use (Gao et al., 2020; Li et al., 2020a). Approximately 80–85% of wheat protein is gluten protein, which is a key component in determining the function of wheat dough, and gluten protein is composed mainly of glutenin and gliadin (Gao et al., 2020; Goesaert et al., 2005; Laidig et al., 2017). Gluten is formed by HMW-GSs and LMW-GSs through disulfide bonds in the gluten network structure. HMW-GSs are the main influencing factor of gluten elasticity and function and play a key role in food processing (Delcour et al., 2012; Gao et al., 2016). Similarly, the elasticity of dough is positively correlated with the content of β-sheets but negatively correlated with that of α-helices (Georget and Belton, 2006). During the mixing process of dough, gluten proteins form a three-dimensional network of wrapped starch granules (Lyu et al., 2022; Singh and MacRitchie, 2001), which determines the viscoelasticity of the dough (Gao et al., 2020; Yu et al., 2022). However, it is not clear whether the regulation of the quality response to sowing date is related to gluten structure, gluten subunit composition, and dough microstructure.

Therefore, four wheat varieties with different grain qualities were selected for this study. Various sowing treatments were established to measure nitrogen accumulation and remobilization, gluten secondary structure, dough microstructure, and gluten subunits in wheat. The objectives of this study were to clarify (1) how sowing dates affected the grain yield and quality of different wheat varieties and (2) whether the effects of sowing date on wheat grain quality were regulated through temperature-mediated plant nitrogen accumulation and reactivation pathways. This study aims to provide new insights into the mechanisms through which sowing date influences wheat yield and quality.

2. Materials and methods

2.1. Experimental design and crop management

The experiment was conducted at the Doukou Crop Experimental Demonstration Station of Northwest A & F University (108°52′ E, 34°36′ N) during the wheat growth seasons of 2020–2021 and 2021–2022. The soil was classified as clay loam with a pH of 8.47. The top 30 cm of soil contained 13.72 g kg^{-1} organic matter, 1.36 g kg^{-1} total nitrogen, 24.92 mg kg^{-1} available nitrogen, 20.18 mg kg^{-1} available phosphorus, and 271.32 mg kg^{-1} available potassium. Meteorological data for the wheat growing seasons from 2020 to 2022 are presented in Fig. 1, with total precipitation of 256.0 mm and 111.7 mm for each season, respectively.

Four wheat varieties were used in this study: two strong-gluten varieties, Xinong20 (XN20) and Weilong169 (WL169), and two medium-gluten varieties, Xiaoyan22 (XY22) and Weilong121 (WL121). Specific varietal characteristics are provided in Table S1. The experiment was initiated in 2020–2021 and included three sowing dates: T1 (October 8), T2 (October 20), and T3 (November 1). T2 was the local conventional sowing date. Results from the first year indicated that early sowing reduced yield and quality, whereas late sowing positively impacted quality. To further investigate the effects of late sowing and continuous rainfall during sowing, the sowing dates were adjusted to T2 (October 20), T3 (November 1), and T4 (November 13) in 2021–2022.

The experiment followed a split-plot design, with sowing date as the main plot and wheat variety as the subplot. There were 12 treatment combinations, each replicated three times, resulting in 36 plots measuring 4 m × 4 m each. Wheat was drilled in rows spaced 25 cm apart at a seeding rate of 3.3×10^6 seeds ha^{-1}, following local farmers' common practices. Fertilizers, including urea and diammonium phosphate, were applied before sowing winter wheat, providing 180 kg ha^{-1} of nitrogen (N) and 90 kg ha^{-1} of phosphorus (P_2O_5). Water management employed local conventional microsprinkler irrigation during the wintering and jointing periods, with each irrigation amounting to 100 mm. Weed control was carried out at the five-leaf stage using a 3% mesosulfuron-methyl oil suspension agent (450 mL ha^{-1}). For pest and disease management, applications of 10% imidacloprid (300 g ha^{-1}), 50% carbendazim (900 mL ha^{-1}), 15% triadimefon wettable powder (1,125 g ha^{-1}), and 4.5% cypermethrin (750 mL ha^{-1}) were made at the jointing and flowering stages. All management practices followed local high-yield protocols to ensure that crop growth was not limited by factors other than the sowing date treatment.

2.2. Sampling and measurement

2.2.1. Growing degree days (GDD)

GDD after sowing were calculated by summing the daily average temperatures, using the formula [(Tmax + Tmin)/2], assuming a base temperature of 0°C.

2.2.2. Yield and yield components

To measure yield and yield components, three 1 m^2 areas of wheat plants were randomly harvested from each plot at maturity. After counting the number of spikes per unit area, ten spikes were randomly selected from each sample to record the number of grains per spike. After threshing, the thousand-grain weight and the total weight of all seeds from each sample were measured to calculate the actual yield. The moisture content of the wheat seeds was measured using a grain moisture meter (LDS-1G, Shanghai Qingpu Oasis Testing Instrument Co.,

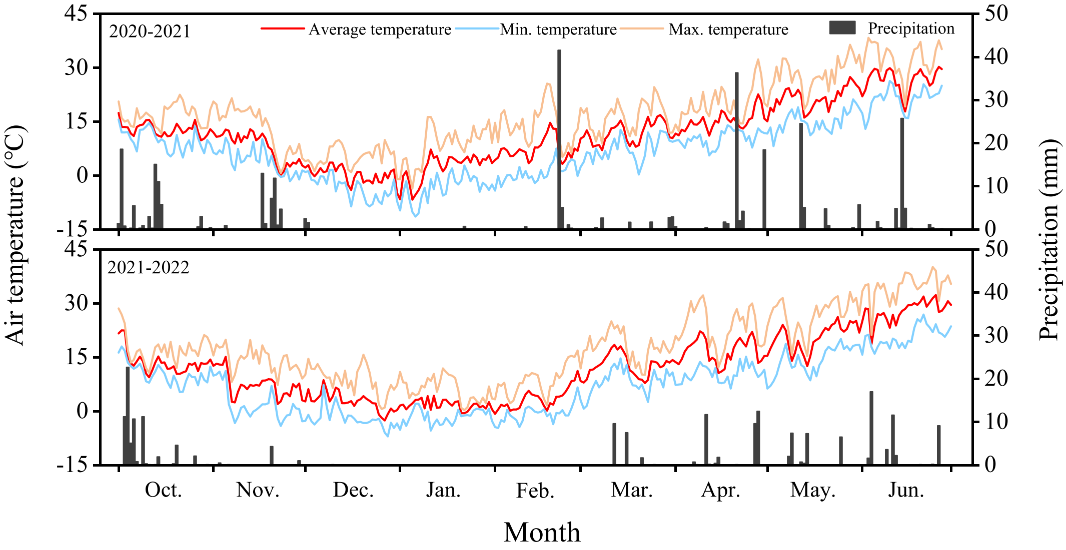

Fig. 1. Daily average, minimum, and maximum temperatures, along with precipitation at the experimental site during the winter wheat growing seasons of 2020–2021 and 2021–2022.

Ltd., Shanghai, China). The actual yield for all treatments was standardized to a moisture content of 13.5%.

2.2.3. *Distribution and remobilization of nitrogen*

To determine the nitrogen distribution and remobilization of wheat plants, 50 cm long winter wheat plants in one row were selected from each plot at flowering and maturity stages. The roots of these plants were severed, and the above-ground portions were harvested. These plant samples were initially heated at 105°C for 30 min to kill the tissue and then dried at 80°C until a constant weight was achieved. Subsequently, the samples were weighed, crushed, and sieved through a 100-mesh screen. The nitrogen content of the processed samples was then determined using continuous-flow analysis (AA3, SEAL) (Zhang et al., 2022b).

$$\text{N accumulation at the flowering stage (NAA)} = \text{the sum of the N accumulated in each part during the flowering stage}$$

$$\text{N accumulation at the maturity stage (NAM)} = \text{the sum of the N accumulated in each part during the maturity stage}$$

$$\text{Nitrogen accumulation in straw at maturity stage (NAVM)} = \text{NAM} - \text{N accumulation in grains (NAG)}$$

$$\text{The N remobilization amount (NRA)} = \text{NAA} - \text{NAVM}$$

$$\text{The N remobilization rate (NRR)} = \text{NRA}/\text{NAA}$$

$$\text{The total contribution rate of N remobilization preflowering to grain N (NRCT)} = \text{NRA}/\text{NAG}$$

For further analysis, the measured values of NAA, plant nitrogen content at flowering (PNC), grain protein content (PC), NRA, and NRR for each variety under different sowing dates were normalized. Specifically, the values obtained for T1, T3, and T4 were divided by the mean value of T2, yielding the relative nitrogen accumulation in plants at wheat flowering (RNAA), relative plant nitrogen content at flowering (RPNC), relative grain protein content (RPC), relative nitrogen remobilization amount (RNRA), and relative nitrogen remobilization rate (RNRR).

2.2.4. *Flour preparation*

To obtain the test flour, the harvested wheat grains were first stored in a cool and dry place for two months after harvest, and then the moisture content was adjusted to 15%. The samples were subsequently ground using a laboratory mill (FW-200AD, Tianjin Xinbode Instrument Co., Ltd.). The whole wheat flour obtained by crushing the grain and passing through a 100-mesh sieve was stored in a refrigerator at 4°C for testing.

2.2.5. *Parameters related to wheat grain quality and dough mixing characteristics*

The protein content, wet gluten content, sedimentation value, and extensibility of the wheat grains were determined using a near-infrared spectrometer (DiodeArray 7250, Perten Instruments, Huddinge, Sweden). The wavelength range is 950 nm–1,650 nm, and the wavelength accuracy is less than 0.3 nm. The dough formation time and stabilization time were measured with a Mixolab (Mixolab 2, Chopin Technologies, France).

2.2.6. *Wheat protein components*

The extraction procedure was adapted from Lyu et al. (2022). Briefly, 0.2 g of wheat flour was placed in a 10 mL centrifuge tube, mixed with 5 mL of distilled water, and incubated at 50°C for 30 min. After centrifugation at 5,000 × g for 30 min, the supernatant was transferred to a new container. Another 5 mL of distilled water was added to the remaining precipitate in the centrifuge tube, and the extraction steps were repeated. The combined supernatants were used to determine the serum albumin concentration. Next, 5 mL of a 5% (w/v) NaCl solution was added to the remaining mixture, which was subsequently incubated at 25°C for 30 min and centrifuged at 5,000 × g for 30 min. The supernatant was retained, and the extraction steps were repeated for globulin determination. Subsequently, 5 mL of 75% (v/v) ethanol was added to the remaining substance, which was subsequently incubated at 25°C for 30 min and centrifuged at 5,000 × g for 30 min. The supernatant was transferred, and the extraction steps were repeated. Finally, the remaining material was mixed with 5 mL of 0.2% (w/v) NaOH (pH 11), incubated at 30°C for 30 min, and centrifuged at 5,000 × g for 30 min. The supernatant was collected, and the extraction steps were repeated for glutenin determination. The protein content of the extracted components was calculated using the Kjeldahl method, with the nitrogen content multiplied by a coefficient of 5.7. Each test was conducted in triplicate.

2.2.7. Quantification of HMW-GSs and LMW-GSs

HMW-GSs and LMW-GSs were extracted according to previously established methods (Gao et al., 2012). First, 50 mg of flour was dissolved in 1 mL of 50% n-propanol solution and incubated in a water bath at 65°C for 20 min. After incubation, the mixture was centrifuged at 16,250 × g for 10 min, retaining the precipitate and discarding the supernatant. Next, 100 μL of an extraction buffer containing 1% dithiothreitol, 80 mM Tris-HCl (pH 8.0), 2% SDS, and 50% n-propanol was added to the precipitate, followed by incubation at 65°C for 30 min. Subsequently, 100 μL of an extraction buffer containing 1% 4-vinylpyridine, 80 mM Tris-HCl (pH 8.0), 2% SDS, and 50% n-propanol was added, and the mixture was incubated at 65°C for 15 min. After centrifugation at 16,250 × g for 5 min, the supernatant containing the protein was transferred to a new centrifuge tube. Finally, 100 μL of buffer containing 80 mM Tris-HCl (pH 8.0), 0.2% SDS, 20% glycerol, and 0.02% bromophenol blue was added. The mixture was incubated at 100°C for 5 min and centrifuged at 16,250 × g for 5 min. The supernatant was subjected to SDS-PAGE using an SDS-PAGE gel preparation kit (Coolaber). The contents of each HMW-GSs and LMW-GSs in each lane were quantified using ImageJ (Fiji, Version 1.52®, NIH; https://imagej.net/software/imagej) analysis software (Zhong et al., 2018).

2.2.8. Disulfide bonds

Ellman's reagent colorimetry was utilized and adapted following the methods of Beveridge et al. (1974) and Guo et al. (2018). Fifty mg of the prepared gluten powder was dissolved in 10 mL of Tris-glycine buffer (pH 8.0, containing 8 M urea, 3 mM EDTA, and 1% SDS), stirred at room temperature for 1 h, and then centrifuged at 13,600 × g for 10 min. The supernatant was retained. First, 0.1 mL of 10 mM DTNB was added to 4 mL of the supernatant and mixed at room temperature. After standing for 20 min, the absorbance was measured at 412 nm to calculate the content of free sulfhydryl groups (-SH_{free}). Subsequently, 1 mL of the supernatant was mixed with 0.1 mL of β-mercaptoethanol and 4 mL of Tris-glycine buffer (pH 8.0, containing 8 M urea, 3 mM EDTA, and 1% SDS). The mixture was left to stand at room temperature for 1 h. After centrifugation at 5,000 × g for 10 min, the precipitate was retained, and the procedure was repeated three times. All collected precipitates were dissolved in 10 mL of Tris-glycine buffer (pH 8.0, containing 8 M urea, 3 mM EDTA, and 1% SDS). After adding 0.1 mL of DTNB, the absorbance was recorded at 412 nm to determine the total sulfhydryl ($\text{-SH}_{\text{total}}$) content. The disulfide bond content was calculated as $(\text{-S-S-}) = 1/2\,(\text{-SH}_{\text{total}} - \text{-SH}_{\text{free}})$.

2.2.9. Gluten secondary structure

The secondary structure of gluten was determined using the methods described by Li et al. (2020b). The samples were characterized using a Fourier transform spectrometer (Vertex70, Bruker, Germany). The secondary structure was analyzed in the amide I region (1,600–1,700 cm^{-1}) with Omnic software (Omnic Specta 8.0, Thermo Scientific, USA) and PeakFit software (PeakFit v4.12, SeaSolve Software Inc., USA). Specifically, the intermolecular β-sheet was identified in the 1,613–1,620 cm^{-1} range, the intramolecular β-sheet was identified in the 1,627–1,635 cm^{-1} range, and the α-helix was identified in the 1,650–1,660 cm^{-1} range. The content of each secondary structure was calculated as the ratio of the corresponding peak area to the total peak area.

2.2.10. Dough microstructure

A confocal laser scanning microscope (Leica TCS SP8, Germany) was used to visualize the protein network structure of wheat dough. The method was adapted from Bernklau et al. (2016). The dough was stained with rhodamine B dye solution (0.01 mg mL^{-1}) and examined under excitation light of 559 nm using a 20× magnification objective. Five images were captured for each sample, each with a resolution of 1,024 × 1,024 pixels and a field size of 290.62 μm × 290.62 μm. Following the procedure described by Bernklau et al. (2016), AngioTool64 version 0.6a software (National Cancer Institute, National Institute of Health, Maryland, USA) was employed to process and analyze the images.

2.3. Data analysis

Data organization was performed using Microsoft Excel (Microsoft Corp., Redmond, WA, USA), while SPSS 26.0 (SPSS Inc., Chicago, IL, USA) was used for data analysis. Statistical analysis was performed using a two-way split-plot ANOVA, followed by Fisher's Least Significant Difference (LSD) test for post-hoc multiple comparisons. The significance levels were set at $P < 0.05$ and $P < 0.01$ (LSD 0.05 and LSD 0.01). Finally, data visualization and plotting were carried out using Origin 2021 software (OriginLab Corporation, Northampton, MA, USA) and Microsoft Excel (Microsoft Corp., Redmond, WA, USA).

3. Results

3.1. Phenological development and GDD

The phenological development of wheat was influenced by the sowing date (Fig. 2). Compared to the normal sowing T2, the jointing, heading, and flowering of early sowing T1 were advanced by 4 d, 2 d, and 1–2 d, respectively, while moderate late sowing T3 and late sowing T4 were delayed by 5 d and 11 d, 2–4 d and 4–6 d, and 0–2 d and 1–3 d, respectively. Compared to T2, the average temperature before overwintering for T1 increased by 0.94°C, while the average temperatures from overwintering to jointing, jointing to flowering, and flowering to maturity decreased by 0.44°C, −0.02 to 0.17°C, and 0.15–0.51°C, respectively (Fig. 1). Compared to T2, the average temperatures before overwintering for T3 and T4 decreased by 1.27–1.37°C and 2.11°C, respectively, while the average temperatures from overwintering to jointing, jointing to flowering, and flowering to maturity increased by 0.28–0.32°C and 0.76°C, 0.63–0.86°C and 1.35–1.43°C, and −0.21 to 0.57°C and −0.24 to 0.01°C, respectively. The increase in temperature after jointing accelerated the phenological development of late-sown wheat (Figs. 1, 2). These changes in temperature conditions and wheat phenological development resulted in the primary impact of sowing date on wheat GDD before overwintering (Fig. 3). The difference in GDD between the earliest and latest sowing dates over the two years ranged from 272.51 to 318.75°C d, while the difference in GDD gradually decreased after overwintering. From the flowering stage to maturity, compared to T2, T3, and T4 differed by −80.60 to 22.40°C d and −122.75 to −89.95°C d in GDD, respectively.

3.2. Yield and yield components

The grain yield of wheat was significantly influenced by the sowing date (Table 1). With the delay of sowing date, the yield in 2020–2021 increased first and then decreased, and the yield in 2021–2022 continued to decrease from T2 to T4. The highest yield for both seasons was achieved with T2 except for XN20 in 2020–2021, indicating that October 20 is an optimal sowing date for local wheat. The responses of the three yield components to sowing dates varied. The number of spikes per ha first increased and then decreased with late sowing in 2020–2021, and consistently decreased with late sowing in 2021–2022. Conversely, the number of grains per spike increased with late sowing in both years, while the differences in 1,000-grain weight among the sowing dates were not significant. Significant differences were observed in the response of spike numbers per unit area to the sowing date among the four wheat varieties. T2 produced the highest spike numbers per unit area in both seasons. Compared to T2, the spike numbers per unit area

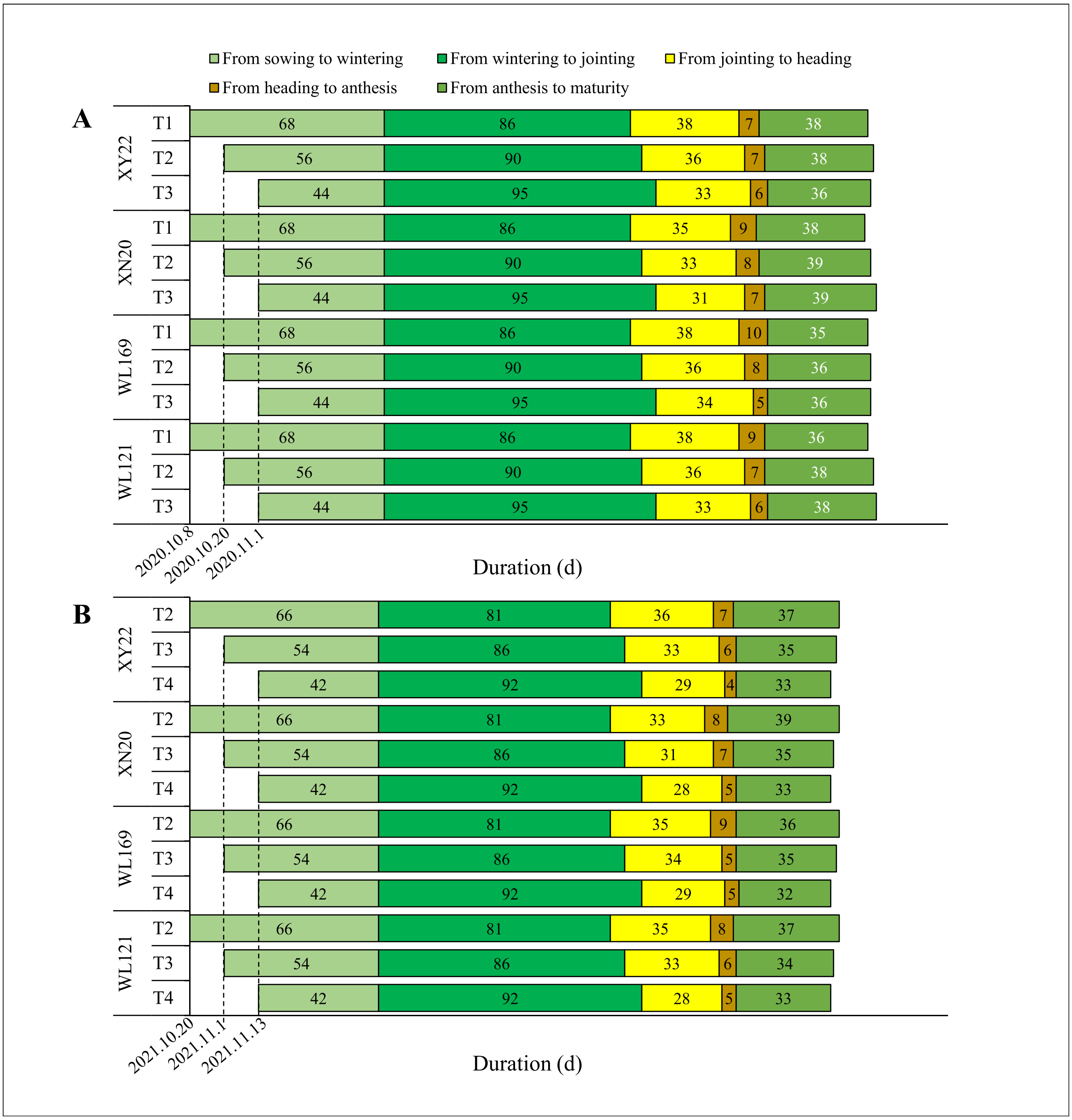

Fig. 2. The effect of sowing date (T1-T4) on the durations of different growth stages for four wheat varieties in 2020–2021 (A) and 2021–2022 (B). Abbrevations: T1, sowing date on October 8; T2, sowing date on October 20; T3, sowing date on November 1; T4, sowing date on November 13; XN20, Xinong20; WL169, Weilong169; XY22, Xiaoyan22; and WL121, Weilong121.

for XY22, XN20, WL169, and WL121 decreased by 10.04%–21.71%, 3.40%–21.55%, 7.72%–25.64%, and 2.85%–18.81%, respectively, under the other sowing dates. The sensitivity of spike numbers per ha to the sowing date was lower for WL121 and XN20 compared to XY22 and WL169.

3.3. *Related parameters of wheat grain quality and dough mixing characteristics*

The grain quality and dough mixing characteristics of wheat were influenced by the sowing date and its interaction with varieties (Table 2). The protein content, protein yield, wet gluten content, sedimentation value, extensibility, and dough stabilization time of wheat grains increased with the late sowing date in 2020–2021. In 2021–2022, these values initially increased but then decreased, reaching their maximum at T3 in both years. Compared to other sowing dates, the increases observed at T3 ranged from 1.71% to 27.22% for protein content, 3.32% to 15.42% for protein yield, 1.18%–20.97% for wet gluten content, −1.13% to 57.36% for sedimentation value, 0.74%–23.46% for extensibility, and 2.01%–34.29% for dough stabilization time. For the same sowing date, the strong-gluten varieties XN20 and WL169 exhibited superior grain quality and dough mixing characteristics compared to the medium-gluten varieties XY22 and WL121. However, the dough stabilization time of XY22 was not significantly affected by the sowing date.

3.4. *Dough microstructure*

During the 2020–2021 growing season, late sowing resulted in a more uniform protein network structure with smaller pore sizes in the wheat dough (Figs. 4A, 5). This delay led to a significant increase in gluten area, gluten junctions, branching rate, and total gluten length, peaking at T3 (Fig. 5). Conversely, the gluten endpoints and lacunarity decreased. In 2021–2022, the protein network structure at T3 became more complex

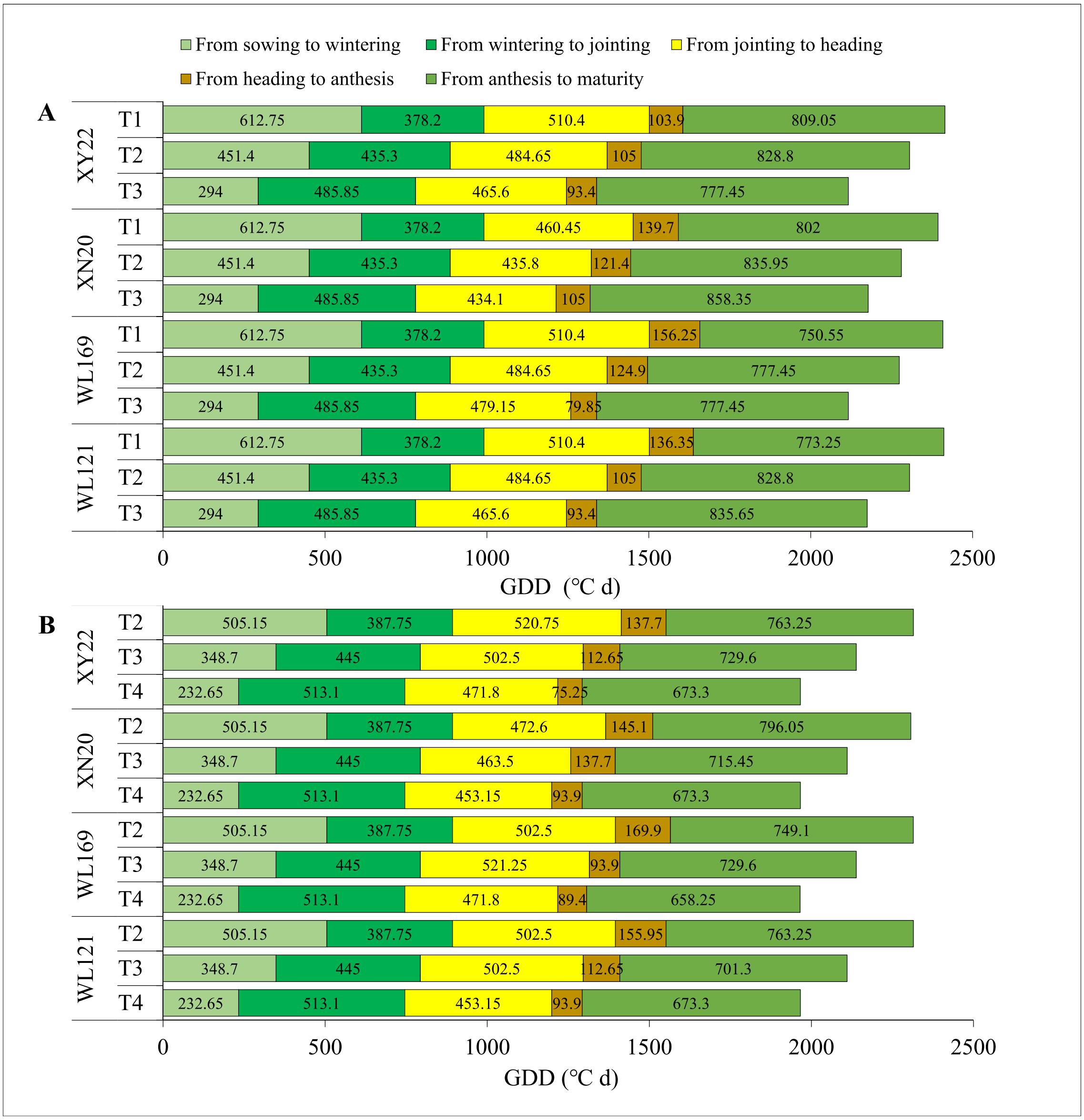

Fig. 3. Effects of sowing date (T1-T4) on cumulative growing degree days (GDD) of different growth stages for four wheat varieties in 2020–2021 (A) and 2021–2022 (B). Abbreviations: T1, sowing date on October 8; T2, sowing date on October 20; T3, sowing date on November 1; T4, sowing date on November 13; XN20, Xinong20; WL169, Weilong169; XY22, Xiaoyan22; and WL121, Weilong121.

with smaller pores (Fig. 4B). Quantitative analysis revealed that in 2021–2022, the gluten area, gluten junctions, junction density, branching rate, and total gluten length peaked at T3, while lacunarity was at their lowest. Additionally, strong-gluten wheat varieties XN20 and WL169 exhibited a more complex and compact protein network structure compared to medium-gluten varieties XY22 and WL121 (Fig. 4).

3.5. Grain protein components

Gliadin and glutenin accounted for 38.09%–44.05% and 40.82%–46.76% of the total protein, respectively (Fig. 6). In 2020–2021, the contents of albumin, globulin, gliadin, and glutenin and ratio of glutenin to gliadin (Glu/Gli) in the four different wheat varieties significantly increased with late sowing. In 2021–2022, their contents first increased but then decreased with late sowing, reaching the maximum at T3 in both years. Over the two-year period, the maximum increases observed at T3 ranged from −0.60% to 36.98% for albumin, 2.98%–54.65% for globulin, 1.49%–15.37% for gliadin, and 10.43%–28.88% for glutenin compared to other sowing dates. Under the same sowing conditions, the strong-gluten varieties XN20 and WL169 had higher protein content than the medium-gluten varieties XY22 and WL121. The allometric scaling equations for grain protein allocation explained 73–93% of the observed variation in protein, gliadin, and glutenin contents per grain. The scaling coefficients in the power function equations indicated that the growth rate of protein was greater than that of grain weight, and there were significant differences in the scaling coefficients between glutenin and gliadin, suggesting that glutenin and gliadin increased disproportionately with protein, with the growth rate of glutenin being significantly higher than that of gliadin.

3.6. HMW-GSs and LMW-GSs

In 2020–2021, the content of HMW-GSs increased significantly with late sowing (Fig. 7). There was no significant difference in LMW-GSs content between T1 and T2; however, the LMW-GSs content at T3 was significantly higher than at T1 and T2. The HMW-GSs and LMW-GSs

Table 1

Effects of sowing date (T1-T4) on the yield and yield components of four wheat varieties in 2020–2021 and 2021–2022.

Variety	Treatment	Spike number ($\times 10^4$ ha^{-1})		Grain number per spike		1,000-grain weight (g)		Grain yield (t ha^{-1})	
		2020–2021	2021–2022	2021–2022	2021–2022	2021–2022	2021–2022	2021–2022	2021–2022
XY22	T1	521.33bc	–	35.73f	–	41.86d	–	7.20bc	–
	T2	594.00a	634.00ab	36.30ef	37.07e	42.16d	45.88def	7.68a	7.95ab
	T3	507.67c	570.33c	38.20b	42.80bc	44.50b	47.24cd	7.11c	7.54c
	T4	–	496.33e	–	44.80ab	–	48.09bc	–	6.57e
XN20	T1	450.94e	–	38.00bc	–	48.61a	–	6.60de	–
	T2	466.81de	625.00b	37.33bcde	37.70e	48.62a	46.96cd	6.26fg	8.16a
	T3	444.89e	507.67de	38.47b	39.50de	49.10a	49.66ab	6.45ef	7.64bc
	T4	–	490.33e	–	41.80cd	–	50.86a	–	7.12d
WL169	T1	518.00c	–	35.60f	–	43.53c	–	6.81d	–
	T2	561.33ab	574.67c	36.70cdef	37.87e	43.89bc	46.53cde	7.41ab	7.56c
	T3	440.00e	469.00e	39.87a	41.60cd	44.36bc	46.66cde	6.51ef	6.99d
	T4	–	427.33f	–	42.53bc	–	47.38cd	–	6.63e
WL121	T1	497.11cd	–	36.47def	–	41.95d	–	5.99gh	–
	T2	525.26bc	664.67a	37.17bcde	38.50e	40.69e	44.39f	6.06gh	8.24a
	T3	510.28c	572.33c	37.77bcd	43.80abc	39.75f	44.93ef	5.89h	7.72bc
	T4	–	539.67cd	–	45.33a	–	44.04f	–	7.09d
ANOVA	T (treatment)	**	**	**	**	ns	ns	*	**
	V (variety)	**	**	*	**	**	**	**	**
	T × V	**	*	*	ns	**	*	**	ns

Different letters in the same column indicate significant differences ($P < 0.05$). * and ** indicate significant differences at the levels of $P < 0.05$ and $P < 0.01$, respectively, and ns is not significant difference.

Abbrevations: T1, sowing date on October 8; T2, sowing date on October 20; T3, sowing date on November 1; T4, sowing date on November 13; XN20, Xinong20; WL169, Weilong169; XY22, Xiaoyan22; and WL121, Weilong121.

contents in WL169 plants decreased in the order of T1 > T3 > T2. In 2021–2022, the HMW-GSs and LMW-GSs in the four wheat varieties initially increased but then decreased with late sowing. These values were significantly greater at T3 compared to T2 and T4, with no significant difference between T2 and T4. These results indicate that the sowing date significantly affects the HMW-GSs and LMW-GSs contents in wheat.

3.7. Gluten secondary structure and disulfide bonds

The contents of intermolecular β-sheet, β-sheet, and α-helix structures, as well as the α-helix/β-sheet ratio, in four wheat varieties were influenced by the sowing date (Fig. 8). In 2020–2021, late sowing resulted in a significant increase in intermolecular β-sheet and β-sheet contents, while α-helix content and the α-helix/β-sheet ratio decreased significantly. Conversely, in 2021–2022, the intermolecular β-sheet and β-sheet contents initially increased but then decreased with late sowing, whereas the α-helix content and the α-helix/β-sheet ratio showed the opposite trend. Additionally, in the first year, disulfide bond content significantly increased with late sowing (Fig. 9). In the second year, disulfide bond content increased initially, but then decreased, peaking in T3 in both years. For the same sowing date, the disulfide bond content in the strong-gluten wheat varieties XN20 and WL169 was higher than in the medium-gluten wheat varieties XY22 and WL121.

3.8. Nitrogen distribution and remobilization

The NRA, NRR, and NRCT of the four wheat varieties significantly differed under different sowing dates (Fig. 10). In 2020–2021, as sowing was delayed, the NAA, NAG, NRA, NRR, and NRCT values of the four wheat varieties increased, reaching their highest values at T3. However, in 2021–2022, after peaking significantly at T3, the NAA, NAG, NRA, NRR, and NRCT began to decrease with further sowing delay (Table S2). This finding indicates that a moderate delay in sowing benefits nitrogen retranslocation in vegetative organs and nitrogen accumulation in grains, but excessive delay has adverse effects. Additionally, there were significant differences in nitrogen accumulation among the wheat varieties. NAA, NAM, NAG, and NRA values were higher in the strong-gluten wheat varieties XN20 and WL169 compared to the medium-gluten varieties XY22 and WL121. Furthermore, the interaction between sowing date and variety significantly affected nitrogen distribution and remobilization. In particular, the nitrogen accumulation and remobilization ability of WL169 differed from those of the other varieties when sowing was delayed. NAA, NAM, and NAG peaked at T2, and began to decrease with late sowing (Fig. 10).

3.9. Analysis of key factors for processing quality

The Mantel test revealed that the meteorological conditions under different sowing dates primarily influenced plant nitrogen accumulation and reactivation, protein and wet gluten contents, and the α-helix/β-sheet ratio, with pre-flowering meteorological conditions being the main factor affecting wheat quality (Fig. 11). The Mantel test indicated that PNC, NRA, and NRR were significantly and positively correlated with protein content, wet gluten content, and extensibility ($P < 0.05$). NAA, PNC, and NRA were significantly and negatively correlated with the α-helix/β-sheet ratio ($P < 0.01$). Protein content was significantly and positively correlated with wet gluten content, extensibility, stabilization time, disulfide bond content, gluten junctions, and branching rate ($P < 0.05$), while it was significantly and negatively correlated with the α-helix/β-sheet ratio and lacunarity ($P < 0.01$). The Glu/Gli was significantly and positively correlated with disulfide bond content, gluten junctions, and branching rate ($P < 0.05$), while it was significantly and negatively correlated with lacunarity ($P < 0.01$). Gluten junctions and branching rate were significantly and positively correlated with extensibility and stabilization time ($P < 0.05$), while lacunarity was significantly and negatively correlated with extensibility and stabilization time ($P < 0.01$).

Therefore, further regression analysis combining meteorological data on RNAA, RPNC, RPC, RNRA, and RNRR revealed that pre-flowering meteorological conditions had a significant linear relationship with RNAA, RPNC, and RPC, while no significant linear relationship was observed from flowering to maturity (Fig. 12). Before wintering, from wintering to jointing, and from jointing to flowering, RNAA and RPC initially increased and then decreased significantly with increasing average and minimum temperatures, and the same trend was observed with increasing GDD before wintering and from overwintering to jointing. Before wintering, RPNC significantly decreased with increasing average temperature within the monitored range, while from overwintering to jointing and from jointing to flowering, RPNC significantly increased with increasing average temperature. The structural equation

Table 2
Effects of sowing date on wheat grain quality and dough mixing characteristics.

Variety	Treatment	Protein content (%)		Protein yield (t ha^{-1})		Wet gluten (%)		Sedimentation value (mL)		Extensibility (mm)		Stabilization time (min)	
		2020–2021	2020–2021	2020–2021	2020–2021	2020–2021	2020–2021	2020–2021	2020–2021	2020–2021	2020–2021	2020–2021	2020–2021
XY22	T1	11.66h	–	0.84de	–	25.74g	–	20.00d	–	116.79j	–	1.92i	–
	T2	12.06g	13.84e	0.93b	1.10cd	26.34f	31.07d	20.11d	29.01e	122.54i	140.20h	2.08i	1.83g
	T3	13.63bc	15.31b	0.97a	1.16bc	29.66c	34.8b	25.40c	35.19c	137.21f	169.89e	2.23i	2.04g
	T4	–	14.33cd	–	0.94f	–	32.22c	–	31.48d	–	152.97f	–	1.96g
XN20	T1	12.27f	–	0.81ef	–	27.99e	–	20.80d	–	145.84e	–	7.11de	–
	T2	13.16d	14.65c	0.82de	1.20ab	29.25d	31.94c	25.32c	30.62d	155.27d	155.62f	7.39cd	8.97b
	T3	15.61a	16.38a	1.07a	1.25a	33.86a	36.61a	32.73a	39.27a	178.50a	192.12a	7.86b	9.15ab
	T4	–	15.26b	–	1.07d	–	34.78b	–	36.58b	–	182.04d	–	8.03c
WL169	T1	12.62e	–	0.86cd	–	29.70c	–	25.38c	–	157.20cd	–	6.96e	–
	T2	13.46c	15.21b	1.00a	1.15bc	29.65c	34.58b	28.23b	39.00a	158.44c	186.52bc	7.73bc	6.96d
	T3	13.69b	16.04a	0.89bc	1.12cd	30.16b	35.06b	29.07b	38.56a	160.61b	187.89ab	8.42a	9.30a
	T4	–	15.45b	–	1.02e	–	34.65b	–	38.47a	–	183.44cd	–	7.97c
WL121	T1	11.65h	–	0.70h	–	25.03h	–	20.97d	–	125.16h	–	3.82h	–
	T2	12.23fg	12.38g	0.74g	1.02e	26.34f	28.65f	25.12c	28.28e	133.28g	138.83h	4.53g	6.65e
	T3	13.25d	14.05de	0.78 fg	1.09d	28.28e	31.37d	28.70b	34.04c	144.40e	153.56f	5.13f	6.93d
	T4	–	13.34f	–	0.95f	–	29.61e	–	30.94d	–	147.69g	–	5.75f
ANOVA	T (treatment)	**	**	**	**	**	**	**	**	**	**	**	**
	V (variety)	**	**	**	**	**	**	**	**	**	**	**	**
	T × V	**	*	**	ns	**	**	**	**	**	**	**	**

Different letters in the same column indicate significant differences ($P < 0.05$). * and ** indicate significant differences at the levels of $P < 0.05$ and $P < 0.01$, respectively, and ns is not significant difference. Abbrevations: T1, sowing date on October 8; T2, sowing date on October 20; T3, sowing date on November 1; T4, sowing date on November 13; XN20, Xinong20; WL169, Weilong169; XY22, Xiaoyan22; and WL121, Weilong121.

model demonstrated that plant nitrogen accumulation and translocation had a direct and significantly positive effect on grain protein, and β-sheet contents (Fig. 13A). Furthermore, plant nitrogen accumulation, reactivation, grain protein, glutenin, and HMW-GSs directly and significantly influenced the microstructure of dough. Standardized effect analysis indicated that plant nitrogen accumulation and reactivation primarily regulated wheat quality indirectly, while protein content had a direct and predominant influence on wheat quality (Fig. 13B).

4. Discussion

4.1. Relationship of nitrogen distribution and remobilization with sowing date

In this study, the nitrogen content in aboveground plants at flowering tended to increase with late sowing, while nitrogen accumulation in these plants at flowering increased with late sowing in the first year and initially increased before decreasing in the second year, with both years reaching their zenith at T3 (Table S2). The critical period for nitrogen uptake in wheat spans from overwintering to flowering, where the increase in average temperature due to late sowing fosters nitrogen uptake by the plants, increasing the nitrogen content at the flowering stage (Cai et al., 2016; Cao et al., 2024; Kong et al., 2023; Yao et al., 2023). Our results showed that from wintering to jointing and from jointing to flowering, RNAA initially increased but then decreased significantly as the average and minimum temperatures increased, as did GDD from wintering to jointing. In contrast, over the same phenophases, RPNC exhibited a significant upward trend with increasing average temperatures (Fig. 12). Previous studies have also reported that a moderate rise in temperature favors increases in nitrate reductase and glutamine synthetase activities (Majláth et al., 2016; Wang et al., 2023a), thereby promoting nitrogen uptake and accumulation in plants. Moreover, late sowing diminishes unproductive tillers, thereby reducing nitrogen competition and consumption (Ma et al., 2018). This suggests that a judicious delay in sowing can offset the reduction in nitrogen accumulation caused by the short vegetative growth period due to late sowing by elevating the average temperature from overwintering to flowering and mitigating intra-population competition. Therefore, a moderate delay in sowing is beneficial for increasing the temperature between wintering and flowering, which accelerates nitrogen uptake and accumulation and increases the plant nitrogen content; however, when sowing is excessively postponed, the additional nitrogen content can no longer compensate for the decline in nitrogen accumulation caused by reduced dry matter accumulation.

Nitrogen remobilization from vegetative organs to grains is triggered by the N demand of developing grains (sinks) and regulated by the source-sink relationship (Kong et al., 2016; Zhang et al., 2012). As sowing was delayed, the NRA and NRR of all four wheat varieties increased progressively, reaching their maxima at T3, and declined with further delay (Table S2), and the grain-to-leaf ratio showed the same trend (Fig. S1). Plants respond to changes in source-sink ratios by increasing the efficiency of source organs, and higher sink intensities can promote nitrogen reactivation (Guitman et al., 1991; Slafer and Savin, 1994; Yang et al., 2016). The increases in NRA and NRR were probably mediated by the higher grain-to-leaf ratio, which modified the source–sink balance, and the larger sink capacity thus promoted the transport of nitrogen into the kernels. An increase in the 1,000-grain weight was observed, further indicating that late sowing may increase storage capacity, thus promoting the transport of carbon, nitrogen, and other substances to grains. Additionally, nitrogen accumulation, distribution, and transport in wheat plants were influenced by both the environment and variety. The NAA, NAG, and NRA of strong-gluten wheat varieties at the flowering and maturity stages were greater than those of medium-gluten wheat varieties, which is consistent with the results of Li et al. (2023).

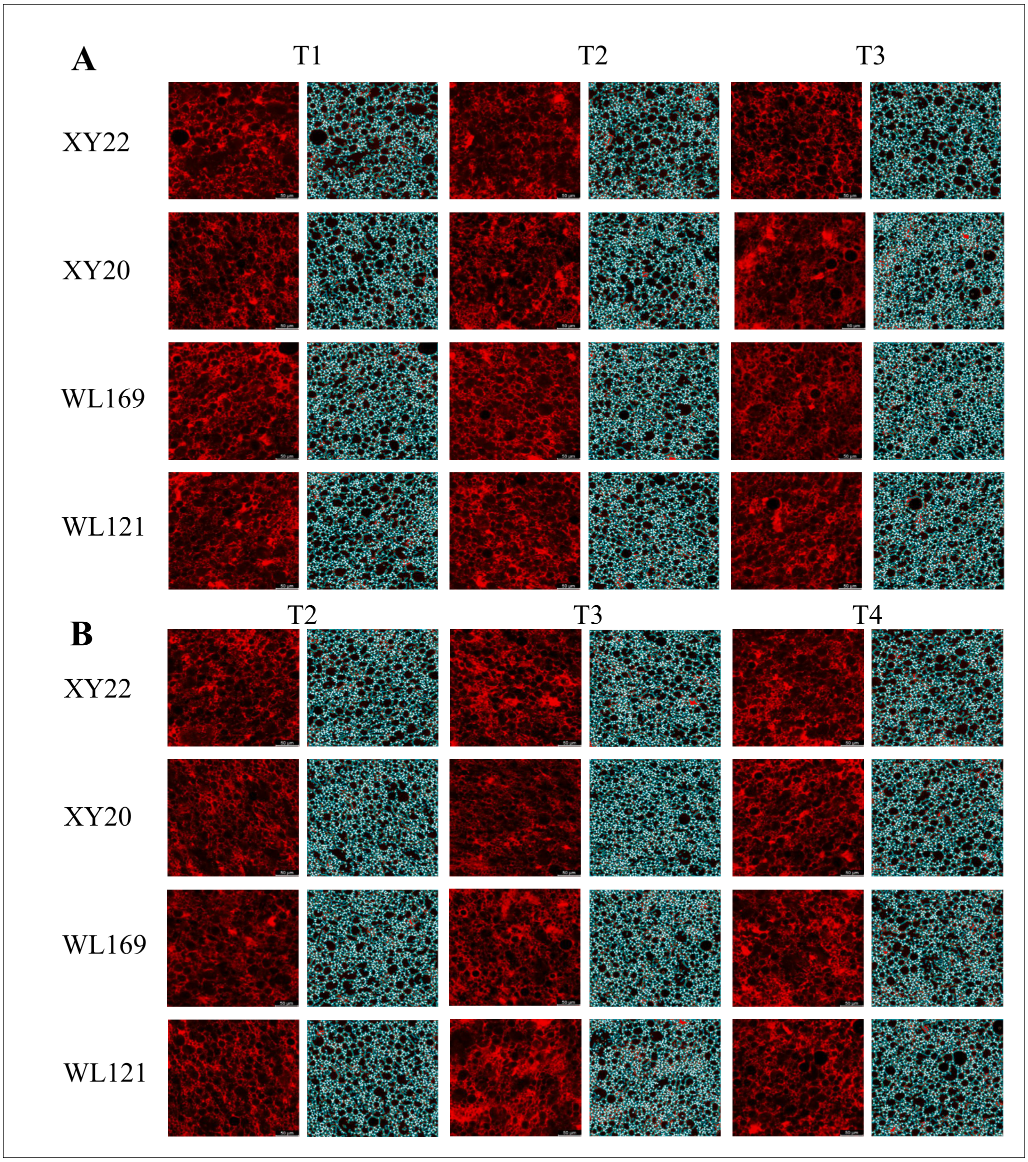

Fig. 4. Protein network analysis of wheat doughs of four wheat varieties grown under different sowing dates (T1-T4) in 2020–2021 (A) and 2021–2022 (B). The first, third, and fifth column images on the left side are original CLSM images, with a scale bar of 50 μm. The second, fourth, and sixth column images on the right side were analyzed using the Angio tool. In these images, the junctions are depicted on white and the protein skeleton is depicted on blue-green. Abbrevations: T1, sowing date on October 8; T2, sowing date on October 20; T3, sowing date on November 1; T4, sowing date on November 13; XN20, Xinong20; WL169, Weilong169; XY22, Xiaoyan22; and WL121, Weilong121.

4.2. Relationships between wheat quality and sowing time

Currently, there is no consensus on how sowing time influences the processing quality of wheat. Some studies suggest that late sowing enhances wheat processing quality (Fois et al., 2011; Li et al., 2013; Mahdavi et al., 2022; Ottaiano et al., 2022; Singh et al., 2021). Conversely, other studies indicated that late sowing either has no effect or diminishes the end-use quality of wheat flour (Dong et al., 2022; Guzmán et al., 2016; Shah et al., 2020). These inconsistencies are likely attributable to variations in trial locations, wheat varieties, and the extent of seeding delays in the experimental designs. Our study revealed that in 2020–2021, protein content, wet gluten content, sedimentation value, extensibility, and dough stabilization time all increased with late sowing. In 2021–2022, these parameters initially increased but then decreased, peaking at sowing time T3. This suggests that while late sowing can improve processing quality to some extent, excessive delays may have adverse effects.

Findings from this two-year study revealed that the protein content in wheat grains increased with late sowing in 2020–2021, whereas it initially increased but then decreased in 2021–2022, peaking at T3 in both years. Adjusting the sowing date appropriately can boost temperatures during the grain-filling phase, curtail the grain-filling period, hasten leaf senescence, and consequently channel more nitrogen into the grains for protein synthesis (Labuschagne et al., 2016; Liu et al., 2016; Lorite et al., 2023; Tao et al., 2018). Nonetheless, the expedited growth process triggered by higher temperatures post-wintering resulted in earlier flowering (Fig. 2), with no significant increase in the average temperature or GDD during the grain-filling period (Fig. 3). Zhu et al. (2023) similarly noted no marked difference in GDD during the grain-filling period for late-sown wheat; hence, grain-filling temperature was not the primary factor behind the variations in grain protein content in this experiment. The protein content in wheat grains is influenced by the nitrogen stored in vegetative organs for remobilization prior to flowering, as well as the nitrogen absorbed by

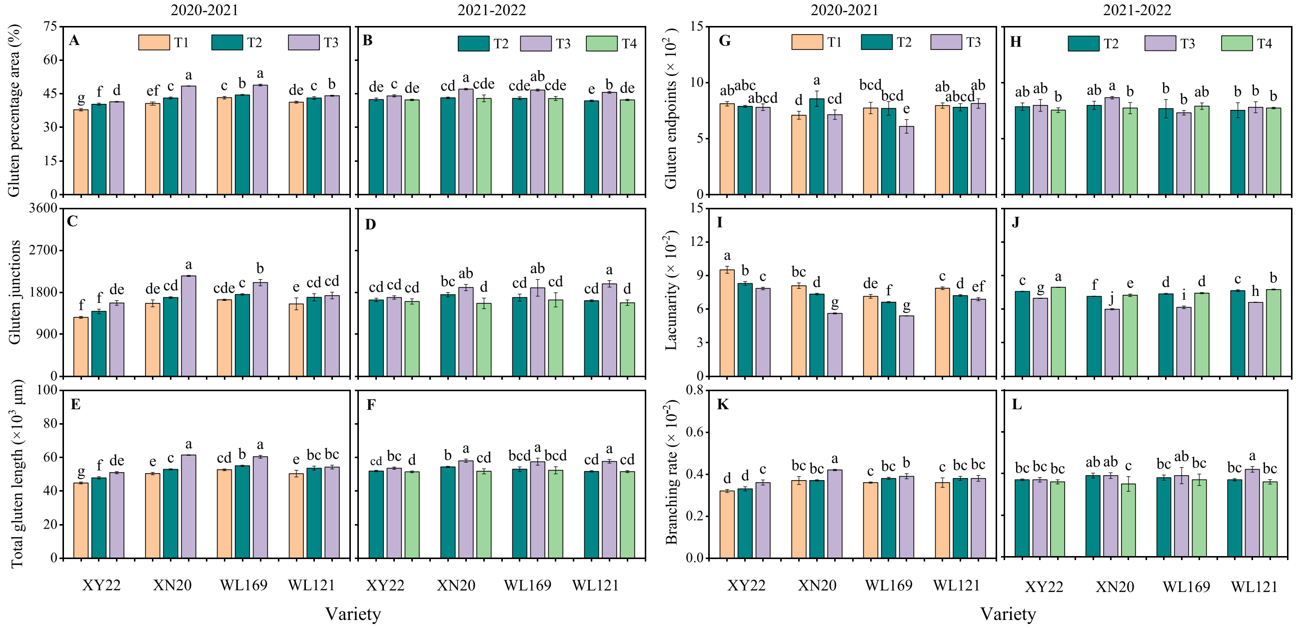

Fig. 5. Effects of sowing date (T1-T4) on wheat dough protein network parameters of four wheat varieties in 2020–2021 and 2021–2022. Vertical bars represent standard deviations of the mean (n = 3). Different letters above the bars within each sub-figure indicate significant differences ($P < 0.05$) among sowing dates and varieties. Abbrevations: T1, sowing date on October 8; T2, sowing date on October 20; T3, sowing date on November 1; T4, sowing date on November 13; XN20, Xinong20; WL169, Weilong169; XY22, Xiaoyan22; and WL121, Weilong121.

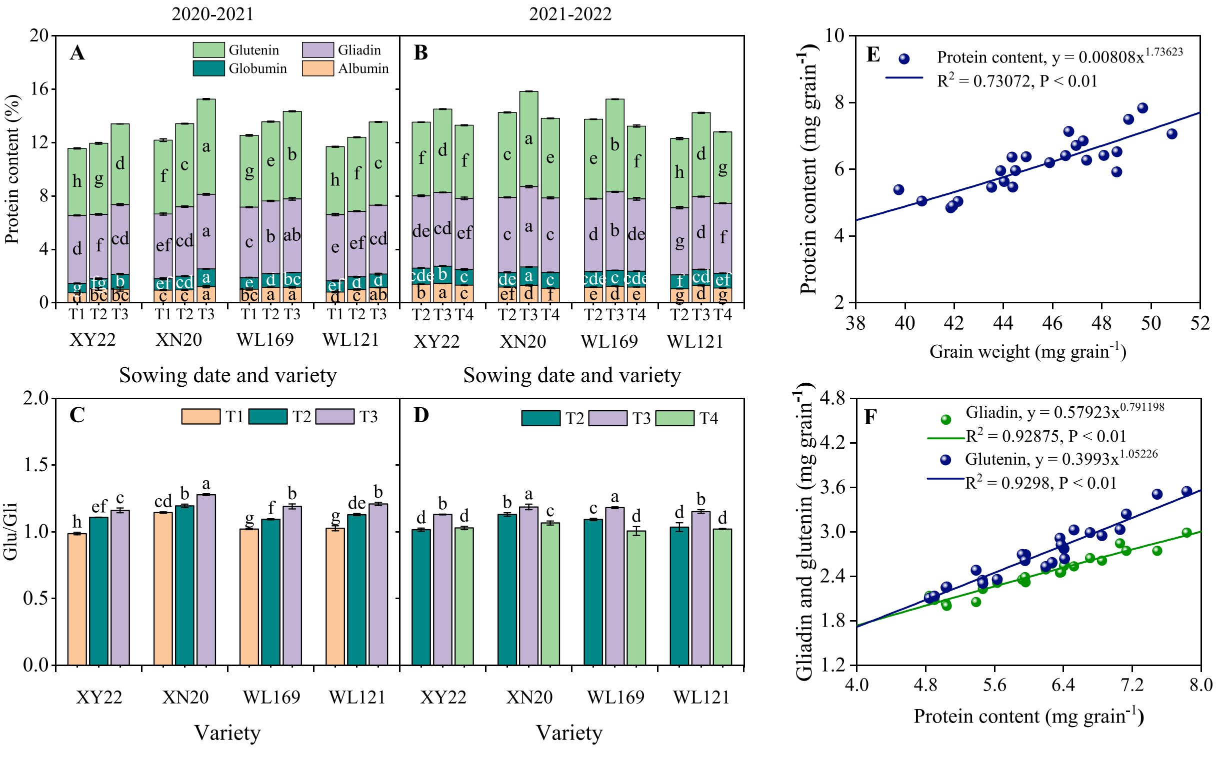

Fig. 6. Effects of sowing date (T1-T4) on the protein components of four wheat varieties in 2020–2021 and 2021–2022. Vertical bars represent standard deviations of the mean (n = 3). Different letters within and above the bars in each sub-figure indicate significant differences ($P < 0.05$) among sowing dates and varieties. Lines are standard major axis regressions of log-transformed data (power function equation). Abbrevations: T1, sowing date on October 8; T2, sowing date on October 20; T3, sowing date on November 1; T4, sowing date on November 13; XN20, Xinong20; WL169, Weilong169; XY22, Xiaoyan22; and WL121, Weilong121.

the plant post-flowering (Ferrise et al., 2010). Enhancing nitrogen uptake and its subsequent remobilization to grains can increase protein content (Dong et al., 2022). In this study, the nitrogen content in aboveground plants at flowering tended to increase with late sowing, while nitrogen accumulation in these plants at flowering increased with late sowing in the first year and initially increased before decreasing in the second year, with both years reaching their zenith at T3 (Table S2). In this study, NAA, PNC, NRA, and NRR were significantly and positively correlated with protein content (Fig. 11). Protein accumulation in grains depends on substrate availability (Fuertes-Mendizábal et al., 2013;

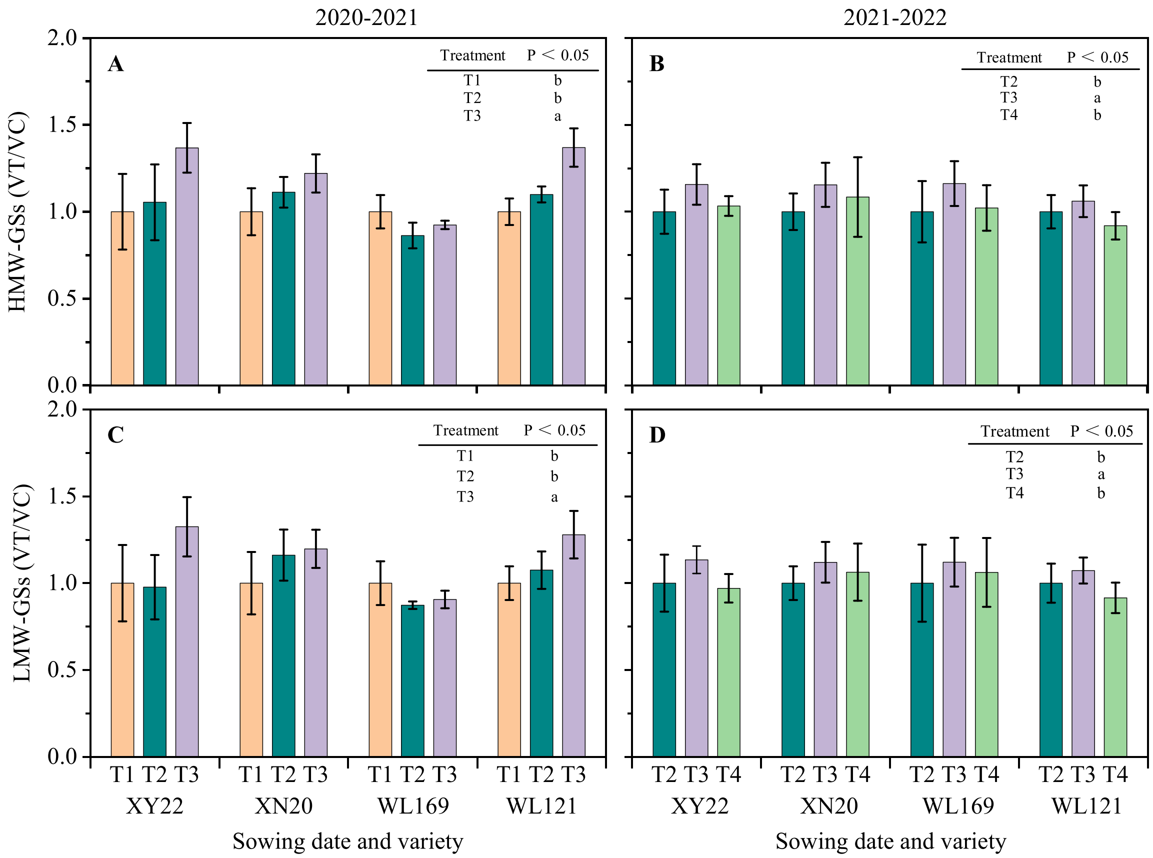

Fig. 7. Effects of sowing date (T1-T4) on high molecular weight glutenins subunits (HMW-GSs, A and B) and low molecular weight glutenins subunits (LMW-GSs, C and D) of four wheat varieties in 2020–2021 and 2021–2022. Results for each variety were normalized to the average values of T2 as the verification control, and T1, T2, T3, and T4 as the verification treatments (T1, T2, T3, or T4 divided by the average value of T2). Vertical bars represent standard deviations of the mean ($n = 3$). The inserted table shows the main factor analysis of variance results from the two-factor split-plot test. Different letters in the inserted table of each panel indicate significant differences among sowing date treatments ($P < 0.05$). Abbrevations: T1, sowing date in October 8; T2, sowing date on October 20; T3, sowing date on November 1; T4, sowing date on November 13; XN20, Xinong20; WL169, Weilong169; XY22, Xiaoyan22; and WL121, Weilong121.

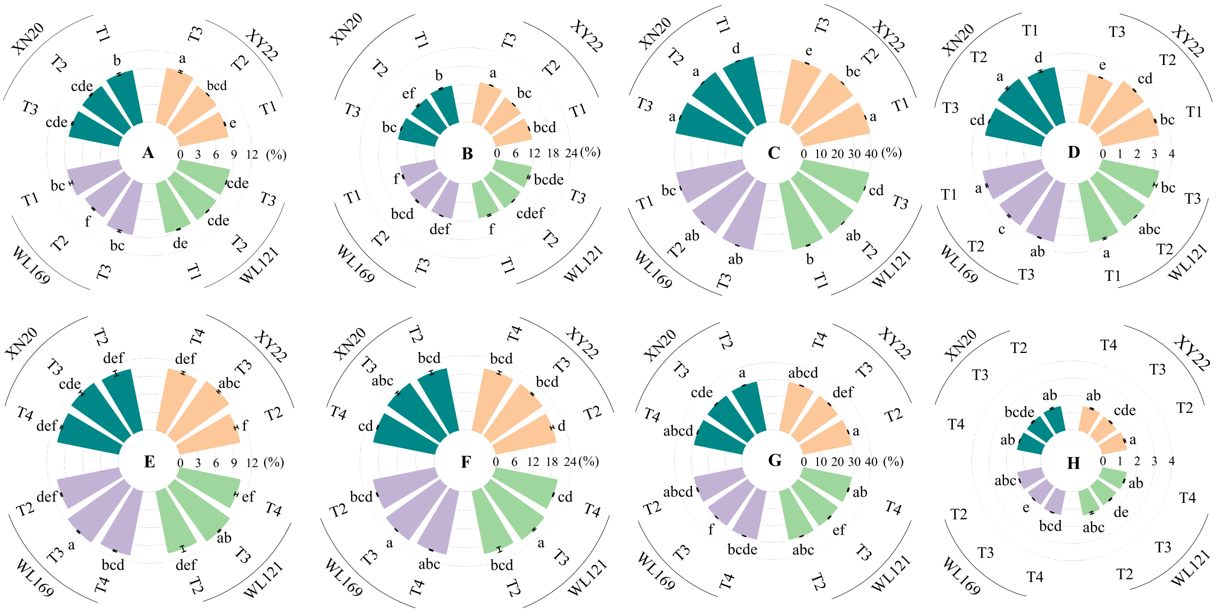

Fig. 8. Effects of sowing date (T1-T4) on the secondary structure of gluten of four wheat varieties. Panels A, B, C, and D show the effects of different sowing dates and varieties on the contents of intermolecular β-sheet, β-sheet, and α-helix and α-helix/β-sheet ratio, respectively, in 2020–2021. Panels E, F, G, and H show the effects of different sowing dates and varieties on the contents of intermolecular β-sheet, β-sheet, and α-helix and α-helix/β-sheet ratio, respectively, in 2021–2022. Vertical bars represent standard deviations of the mean ($n = 3$) Different letters above the bars within each sub-figure indicate significant differences ($P < 0.05$) among sowing dates and varieties. Abbreviations: T1, sowing date on October 8; T2, sowing date on October 20; T3, sowing date on November 1; T4, sowing date on November 13; XN20, Xinong20; WL169, Weilong169; XY22, Xiaoyan22; and WL121, Weilong121.

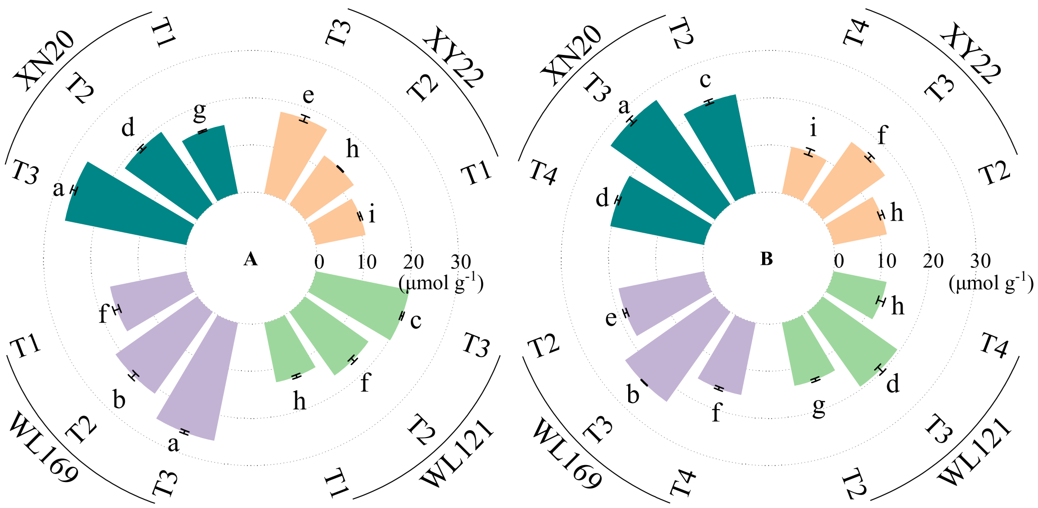

Fig. 9. Effects of sowing date (T1-T4) on disulfide bond content of four wheat varieties in 2020–2021 (A) and 2021–2022 (B). Vertical bars represent standard deviations of the mean (n = 3). Different letters above the bars within each sub-figure indicate significant differences ($P < 0.05$) among sowing dates and varieties. Abbreviations: T1, sowing date on October 8; T2, sowing date on October 20; T3, sowing date on November 1; T4, sowing date on November 13; XN20, Xinong20; WL169, Weilong169; XY22, Xiaoyan22; and WL121, Weilong121.

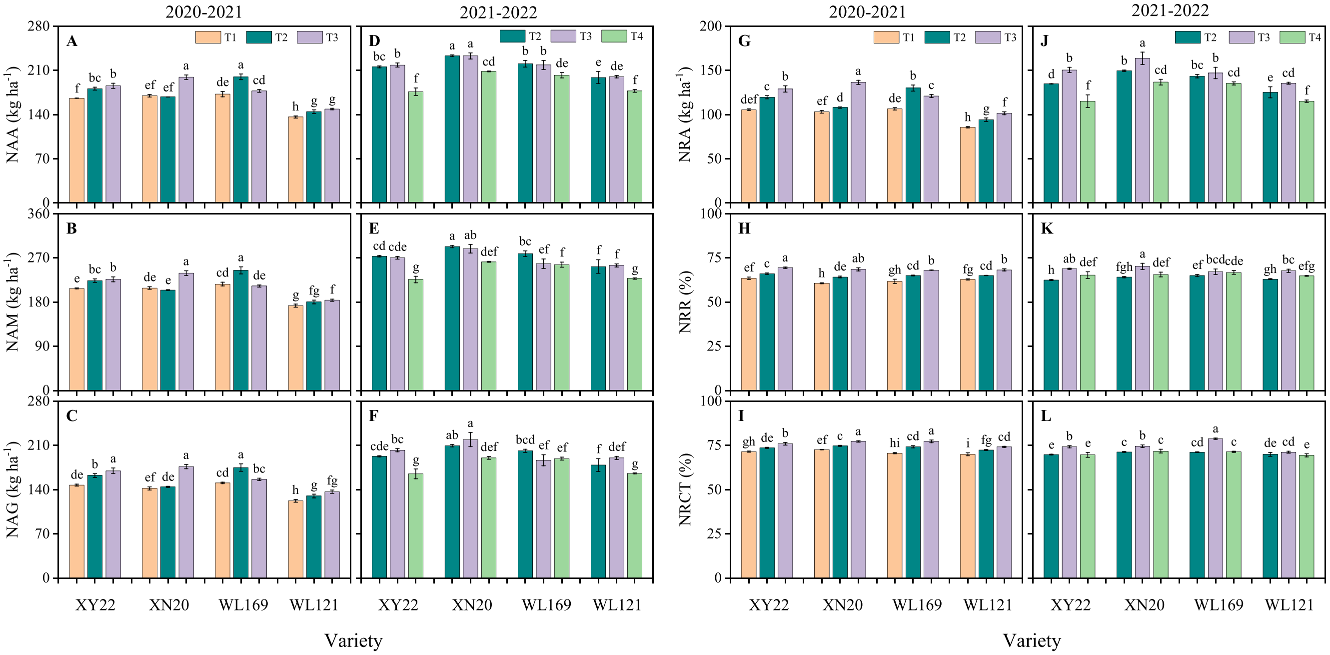

Fig. 10. Effects of sowing date (T1-T4) on nitrogen accumulation, remobilization, and contribution to grain of four wheat varieties in 2020–2021 and 2021–2022. Vertical bars represent standard deviations of the mean (n = 3). Different letters above the bars within each sub-figure indicate significant differences ($P < 0.05$) among sowing date and varieties. Abbreviations: NAA, nitrogen accumulation at flowering; NAM, nitrogen accumulation at maturity; NAG, nitrogen accumulation in grains; NRA, nitrogen remobilization amount; NRR, nitrogen remobilization rate; NRCT, total contribution rate of pre-flowering nitrogen remobilization to grain; T1, sowing date on October 8; T2, sowing date on October 20; T3, sowing date on November 1; T4, sowing date on November 13; XN20, Xinong20; WL169, Weilong169; XY22, Xiaoyan22; and WL121, Weilong121.

Martre et al., 2003), and increasing nitrogen remobilization into the grain can accelerate protein synthesis and accumulation (Chen et al., 2023; Osman et al., 2012). Structural equation modeling further suggests that the increase in grain protein content due to late sowing may result from increased nitrogen accumulation and reactivation (Fig. 13), providing an adequate supply of substrates for protein synthesis and accumulation.

The processing quality of wheat is fundamentally determined by the composition of substances within the grain. To further explore the impact of sowing date on wheat quality, we investigated the microstructure and protein composition. During the mixing of flour with water, gluten proteins form a three-dimensional network around starch granules (Lyu et al., 2022; Singh and MacRitchie, 2001). The primary wheat grain proteins, gliadin and glutenin, combine to form gluten during dough formation. Gliadin interacts with glutenin to enhance the viscosity of the gluten network by reducing the elasticity contributed by glutenin (Delcour et al., 2012; Urade et al., 2018). Consequently, gliadin and glutenin are essential for dough elasticity and mixing tolerance (Delcour et al., 2012). Protein synthesis is primarily constrained by nitrogen availability and increases with higher nitrogen content in the grain (Triboi, 2003). Our study observed that the rate of protein synthesis exceeded that of grain weight, and the synthesis rate of glutenin

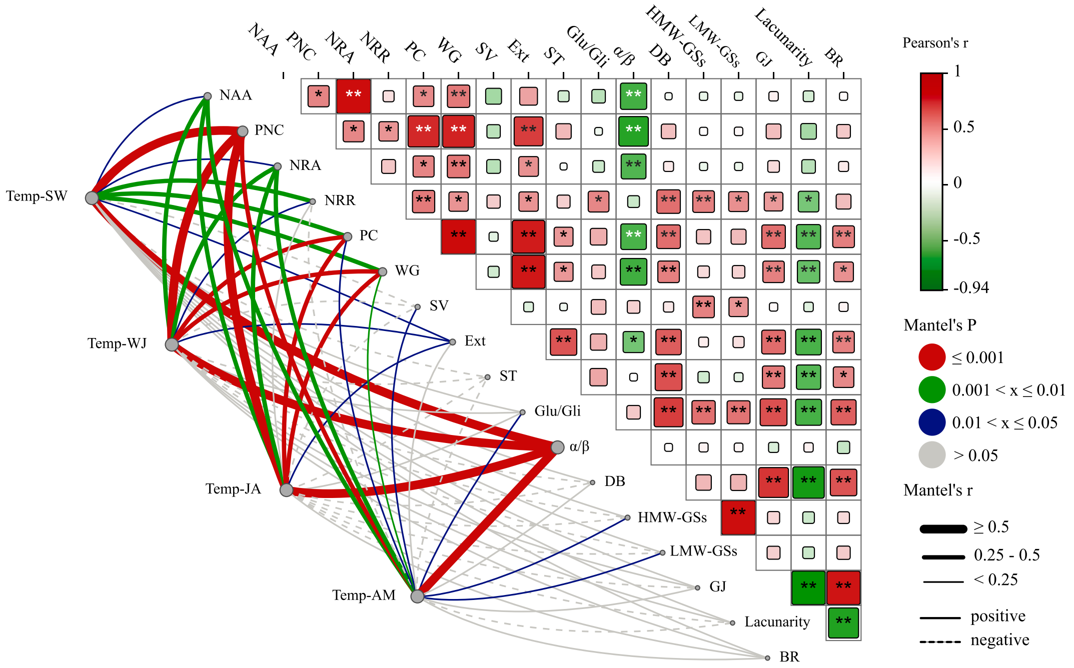

Fig. 11. Mantel tests and Pearson's correlation matrix of wheat dough quality and nitrogen accumulation and translocation. Abbreviations: Temp-SW, before wintering; Temp-WJ, from wintering to jointing, Temp-JA, from jointing to flowering; Temp-AM, from flowering to maturity; NAA, nitrogen accumulation at flowering; PNC, plant nitrogen content at flowering; NRA, nitrogen remobilization amount; NRR, nitrogen remobilization rate; PC, grain protein content; WG, wet gluten content; SV, sedimentation value; Ext, extensibility; ST, stabilization time; Glu/Gli, ratio of glutenin to gliadin; α/β, α-helix/β-sheet ratio; DB, disulfide bonds; HMW-GSs, high molecular weight glutenin subunits; LMW-GSs, low molecular weight glutenin subunits; GJ, gluten junctions (GJ); and BR, branching rate. * and ** indicate significance levels at $P < 0.05$ and $P < 0.01$, respectively.

was significantly higher than that of gliadin and total protein. This resulted in an increased Glu/Gli ratio under appropriately late sowing conditions (Fig. 6), suggesting that late sowing enhances nitrogen remobilization, promotes protein synthesis, and alters Glu/Gli. Gliadins contain intramolecular disulfide bonds and are rich in β-sheet secondary structures (Johansson et al., 2013; Ortolan et al., 2022). Gluten is formed from HMW-GSs and LMW-GSs through disulfide bonding, with HMW-GSs contributing to elasticity (Liu et al., 2022; Shewry et al., 1992). An increased Glu/Gli correlates with a higher proportion of HMW-GSs (Fuertes-Mendizábal et al., 2010), a finding confirmed in our study (Fig. 11). A higher HMW-GS content facilitates the formation of additional disulfide bonds (Fuertes-Mendizábal et al., 2013). The regulation of wheat quality by sowing date may occur through improved nitrogen supply, enhanced protein synthesis and accumulation, increased disulfide bond linkages, changed in protein secondary structure, and improved gluten viscoelasticity (Ding et al., 2023). Our study revealed that late sowing altered the microstructure of dough. Appropriate delays resulted in a more uniform and tightly structured gluten protein network (Fig. 2), attributed to increased disulfide bonds, HMW-GSs, and Glu/Gli, which enhanced gluten cross-linking during dough formation. This led to a more interconnected protein network (Visioli et al., 2018), reduced lacunarity, increased branching rate, and improved distribution of gluten and starch, ultimately enhancing dough stability and quality (Delcour et al., 2012). Dough stabilization time is a reliable indicator of processing quality (MacRitchie, 2016). However, no significant improvement was observed for XY22's dough in either year, which included a less favorable HMW-GSs combination (Bx7+By8) (Fig. S2) (Guo et al., 2022; Guzmán et al., 2022), resulting in a less compact dough structure. Additionally, XY22 exhibited uneven gluten distribution, leading to a loosely connected dough structure (Fig. 4).

4.3. Yield and growth process in relation to sowing date

The yield of wheat is influenced by three primary factors: the number of spikes per unit area, the number of grains per spike, and the weight of 1,000 grains (Fischer, 2008; Prystupa et al., 2004). Competition for radiation, nutrients, and water in wheat creates a trade-off between the number of spikes per unit area and the number of grains per spike (Chen et al., 2008; Dai et al., 2017; Sun et al., 2007). The stability of grain yield in late-sown wheat is maintained by a compensatory relationship between a decrease in spike number per unit area and an increase in the number of grains per spike (Dai et al., 2017; Zhu et al., 2019). This study found that the grain yield of four wheat varieties peaked at T2 across the two years (Table 1), although this trend was not consistent across the two years. In 2020–2021, yield initially increased but then decreased with late sowing, whereas in 2021–2022, yield consistently decreased with late sowing. The primary reason for this discrepancy was that the sowing time in the second year was 12 d later than that in the first year due to continuous rainfall before sowing. The cumulative temperature required for wheat tillering is between 300 and 350°C, with each tiller needing 80–100°C (Ihsan et al., 2016; Sun et al., 2007). Therefore, late sowing beyond the optimal time results in insufficient accumulated temperature before overwintering during the early growth stage, inhibiting tillering (Shah et al., 2020).

In contrast, the number of spikes per unit area at T1 in 2020–2021 was lower than that at T2, likely due to early sowing, which resulted in a high cumulative number of days before winter growth (Fig. 2). This excessive growth period led to tiller production exceeding the optimal number of spikes for maximum yield, causing increased competition for light, water, and nutrients, and resulting in secondary tiller mortality and resource waste (Ma et al., 2018; Zhang et al., 2010). Furthermore, as

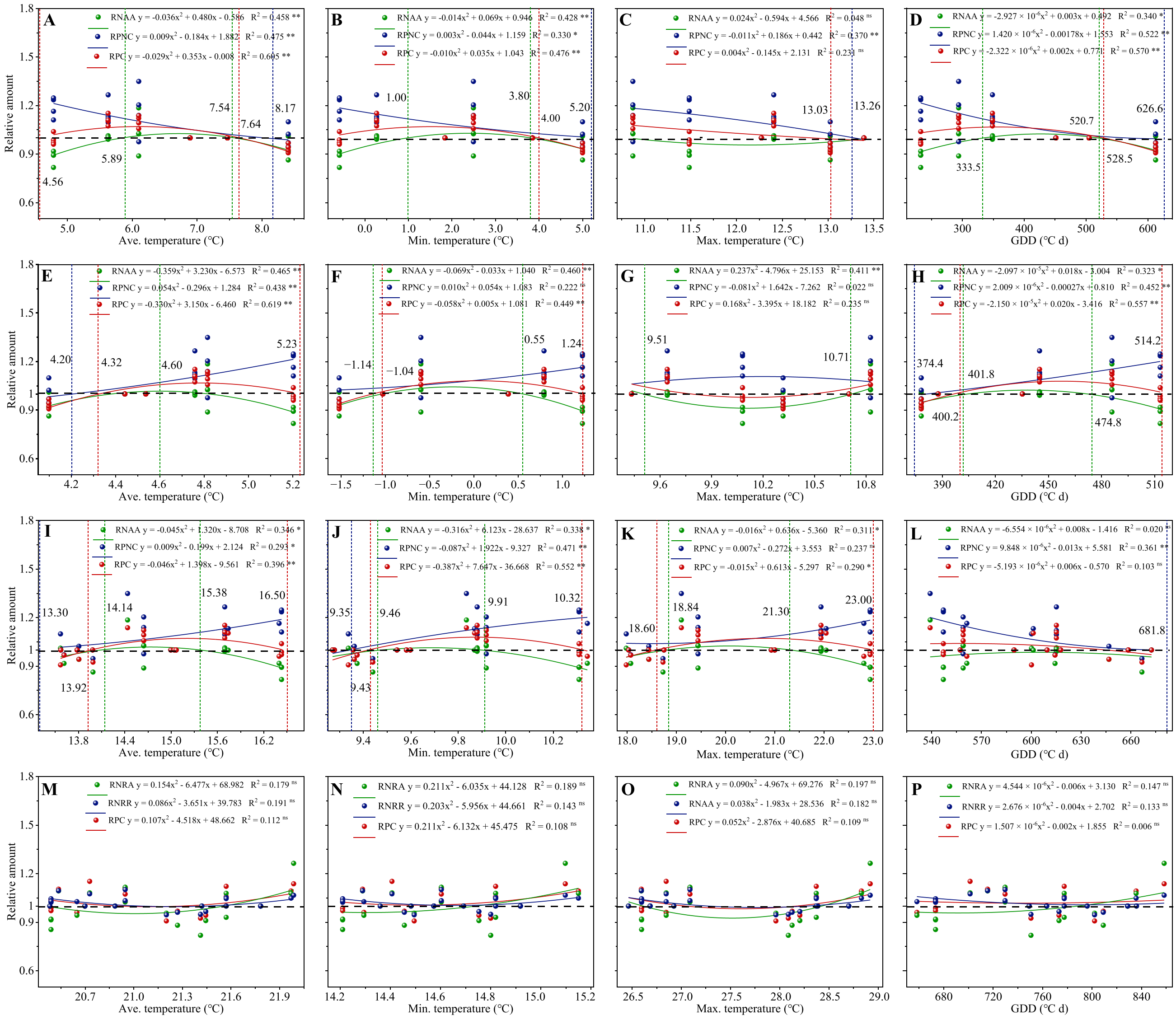

Fig. 12. The relationship of the relative nitrogen accumulation in plants at wheat flowering (RNAA), relative plant nitrogen content at wheat flowering (RPNC), relative grain protein content (RPC), relative nitrogen remobilization amount (RNRA), and relative nitrogen remobilization rate (RNRR) with temperatures before wintering (A–D), from wintering to jointing (E–H), from jointing to flowering (I–L), and from flowering to maturity (M–P). The vertical green, blue, and red dash lines indicate the temperature or growing degree days (GDD) at which RNAA, RPNC, and RPC are 1.0, respectively. * and * indicate significant difference at $P < 0.05$ and $P < 0.05$, respectively, and ns means no significant difference.

global warming increases the frequency of extreme temperatures, the risk of severe frost damage to wheat increases, leading to reduced grains per spike and tillers, thereby decreasing potential grains per unit area and yield (Zheng et al., 2012). The first season of wheat experienced a cold snap on March 20, 2021, which further reduced the number of spikes per unit area and the number of grains per spike for wheat sown at T1, resulting in lower yields. Thus, in the context of global warming, early sowing increases the risk of exposure to extremely low temperatures before and after the booting stage, which is detrimental to achieving high and stable yields.

Additionally, postponing sowing decreased the cumulative growth rate from sowing to wintering (Fig. 2), which may have reduced the number of spikes per ha due to insufficient tillering before winter (Sun et al., 2007). Increased temperatures after overwintering accelerate the wheat growth process, shortening the duration of each developmental stage and leading to earlier flowering in delayed-sown wheat (Sadras and Monzon, 2006; Toyota and Morokuma, 2021; Wang et al., 2023b; Zheng et al., 2012). This was observed in the current study (Fig. 2), but increased temperatures after jointing caused minimal differences in cumulative GDD at each growth stage (Fig. 3). A reduction in tillering can alleviate nutrient competition between stems and spikes, allowing more resources for floral development and increasing the number of grains per spike (Siddique et al., 1989; Zhu et al., 2019). However, late sowing shortens the vegetative growth period, reducing spikelet primordial initiation (Arduini et al., 2018). Consequently, the increase in grains per spike is insufficient to offset the reduction in spikes per unit area, leading to decreased grains per unit area and lower yield. In this study, it was also found that with the delay of sowing date, the number of spikes per unit area decreased, and the number of grains per spike increased (Table 1); however, this increase was not sufficient to compensate for the reduction in the number of spikes per unit area, thereby reducing the total grain yield.

Although the yield of wheat decreased slightly at T3, the protein content and protein yield under appropriate late sowing were the highest, and it was more suitable for making bread according to the standards of General Administration of Quality Supervision, Inspection,

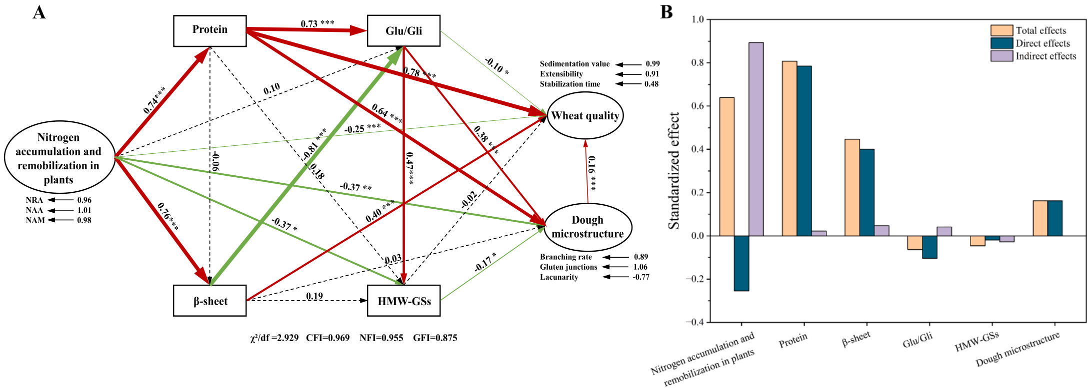

Fig. 13. Structural equation model (SEM) analysis of key factors influencing processing quality. The unidirectional arrows in panel A indicate the hypothesized causal directions. The values shown are standardized path coefficients, indicating positive (red solid line) or negative (green solid line) effects. The black dotted lines denote non-significance effects. The thickness of the solid lines represents the strength of the causal relationships. Panel B displays the results of the path analysis, quantifying the direct and indirect effects that different factors exert on wheat quality standardization in the SEM. *, **, and ** indicate significant differences at the levels of $P < 0.05$, $P < 0.01$, and $P < 0.01$, respectively. Abbreviations: NAA, nitrogen accumulation at flowering; NAM, nitrogen accumulation at maturity; NRA, nitrogen remobilization amount; Glu/Gli, ratio of glutenin to gliadin; HMW-GSs, high molecular weight glutenins subunits; χ^2/df, normed Chi-square; CFI, comparative Fit Index; NFI, normed Fit Index; and GFI, goodness of Fit Index.

and Quarantine of the People's Republic of China (AQSIQ, 2013). The main reason for the decrease in wheat yield caused by late sowing was the decrease in spike number per unit area. Therefore, increasing the late sowing density combined with the improvement of late sowing wheat quality may be an effective way to achieve the production of high-quality wheat in the future.

5. Conclusions

When sowing was postponed to T3, the yield was marginally lower compared to T2, yet there was an improvement in both protein content and quality. The practice of slightly delaying sowing primarily enhanced the temperature conditions from the overwintering phase to flowering, fostered nitrogen uptake and accumulation within wheat plants, and modulated the source-sink dynamics to facilitate nitrogen translocation to the grains, thereby increasing the protein content. Furthermore, this strategic delay in sowing optimized the Glu/Gli ratio, the α-helix/β-sheet ratio, and the formation of disulfide bonds, elevating the relative concentration of HMW-GSs. These improvements bolstered the viscoelastic characteristics of gluten, transformed the dough's microstructure, and elevated the quality of flour processing. The variety played a pivotal role in determining wheat processing quality, with strong-gluten varieties like XN20 and WL169 consistently surpassing medium-strong-gluten varieties such as XY22 and WL121 when sown concurrently. Therefore, considering the trade-off observed in this study between a slight decrease in yield and a significant improvement in protein content and processing quality, we suggest that the period from October 20 to November 1 could be considered a candidate sowing window in this region, with priority given to varieties possessing superior HMW-GS composition.

Abbreviations

BR	branching rate
DB	disulfide bonds
Ext	extensibility
GJ	gluten junctions
Glu/Gli	ratio of glutenin to gliadin
HMW-GSs	high molecular weight glutenin subunits
LMW-GSs	low molecular weight glutenin subunits
NAA	N accumulation at the flowering stage
NAG	N accumulation in grains
NAM	N accumulation at the maturity stage
NAVM	Nitrogen accumulation in vegetative organs at maturity stage
NRA	N remobilization amount
NRCT	total contribution rate of N remobilization preflowering to grain N
NRR	N remobilization rate
PC	grain protein content
PNC	plant nitrogen content at flowering
RNAA	relative nitrogen accumulation in plants at wheat flowering
RNRA	relative nitrogen remobilization amount
RNRR	relative nitrogen remobilization rate
RPC	relative grain protein content
RPNC	relative plant nitrogen content at flowering
ST	stabilization time
SV	sedimentation value
WG	relative wet gluten content
α/β	α-helix/β-sheet ratio

Authors' contributions

Yakun Li: Writing – original draft, Methodology, Data curation. **Xidan Cao:** Validation, Investigation. Jingyi Feng: Software, Investigation. **Huihui Hu:** Formal analysis. **Yi Liu:** Software. Vinay Nangia: Methodology. **Yang Liu:** Conceptualization.

Availability of data and materials

Data will be shared upon request by the readers.

Declaration of competing interest

The authors declare that they have no known competing financial interests or personal relationships that could have appeared to influence the work reported in this paper. Author Yang Liu (Editorial Board member) was not involved in the journal's review or decisions related to this manuscript.

Acknowledgements

This research was supported by the National Key Research and Development Program of China (2024YFD2300205) and the Key Research and Development Program of Shaanxi (2024NC-ZDCYL-01-12).

Appendix A. Supplementary data

Supplementary data to this article can be found online at https://doi.org/10.1016/j.crope.2025.10.001.

References

AQSIQ (General Administration of Quality Supervision, Inspection and Quarantine of the People's Republic of China), 2013. Standardization Administration of the People's Republic of China. GB/T 17320-2013. Standards Press of China, Beijing, China. https://openstd.samr.gov.cn/bzgk/gb/newGbInfo?hcno=BA2618999FD025BFE3D9B82849E3BB4E.

Arduini, I., Pellegrino, E., Ercoli, L., 2018. Contribution of main culm and tillers to grain yield of durum wheat: influence of sowing date and plant traits. Ital. J. Agron. 13, 235–247. https://doi.org/10.4081/ija.2018.1115.

Austin, R.B., Ford, M.A., Edrich, J.A., Blackwell, R.D., 1977. The nitrogen economy of winter wheat. J. Agric. Sci. 88, 159–167. https://doi.org/10.1017/S002185960003389X.

Bernklau, I., Lucas, L., Jekle, M., Becker, T., 2016. Protein network analysis - A new approach for quantifying wheat dough microstructure. Food Res. Int. 89, 812–819. https://doi.org/10.1016/j.foodres.2016.10.012.

Beveridge, T., Toma, S.J., Nakai, S., 1974. Determination of SH- and SS-groups in some food proteins using ellman's reagent. J. Food Sci. 39, 49–51. https://doi.org/10.1111/j.1365-2621.1974.tb00984.x.

Cai, C., Yin, X., He, S., Jiang, W., Si, C., Struik, P.C., Luo, W., Li, G., Xie, Y., Xiong, Y., Pan, G., 2016. Responses of wheat and rice to factorial combinations of ambient and elevated CO_2 and temperature in FACE experiments. Glob. Change Biol. 22, 856–874. https://doi.org/10.1111/gcb.13065.

Cao, Y., Yin, T., Zhang, Y., Yang, X., Liu, B., Zhu, Y., Tang, L., Xiao, L., Cao, W., Liu, L., 2024. Quantitative assessment of the effects of rising temperature on the grain protein of winter wheat in China and its adaptive strategies. Comput. Electron. Agric. 226, 109474. https://doi.org/10.1016/j.compag.2024.109474.

Chen, C., Neill, K., Wichman, D., Westcott, M., 2008. Hard red spring wheat response to row spacing, seeding rate, and nitrogen. Agron. J. 100, 1296–1302. https://doi.org/10.2134/agronj2007.0198.

Chen, Y., Chen, H., Chen, R., Yang, H., Zheng, T., Huang, X., Fan, G., 2023. The impacts of nitrogen accumulation, translocation, and photosynthesis on simultaneous improvements in the grain yield and gluten quality of dryland wheat. Agronomy 13, 1283. https://doi.org/10.3390/agronomy13051283.

Chu, J., Guo, X., Zheng, F., Zhang, X., Dai, X., He, M., 2023. Effect of delayed sowing on grain number, grain weight, and protein concentration of wheat grains at specific positions within spikes. J. Integr. Agric. 22, 2359–2369. https://doi.org/10.1016/j.jia.2023.02.002.

Dai, X., Wang, Y., Dong, X., Qian, T., Yin, L., Dong, S., Chu, J., He, M., 2017. Delayed sowing can increase lodging resistance while maintaining grain yield and nitrogen use efficiency in winter wheat. Crop J. 5, 541–552. https://doi.org/10.1016/j.cj.2017.05.003.

Delcour, J.A., Joye, I.J., Pareyt, B., Wilderjans, E., Brijs, K., Lagrain, B., 2012. Wheat gluten functionality as a quality determinant in cereal-based food products. Annu. Rev. Food Sci. Technol. 3, 469–492. https://doi.org/10.1146/annurev-food-022811-101303.

Ding, J., Hu, H., Yang, J., Wu, T., Sun, X., Fang, Y., Huang, Q., 2023. Mechanistic study of the impact of germinated brown rice flour on gluten network formation, dough properties and bread quality. Innov. Food Sci. Emerg. Technol. 83, 103217. https://doi.org/10.1016/j.ifset.2022.103217.

Dong, S., Zhang, X., Chu, J., Zheng, F., Fei, L., Dai, X., He, M., 2022. Optimized seeding rate and nitrogen topdressing ratio for simultaneous improvement of grain yield and bread-making quality in bread wheat sown on different dates. J. Sci. Food Agric. 102, 360–369. https://doi.org/10.1002/jsfa.11366.

Ferrise, R., Triossi, A., Stratonovitch, P., Bindi, M., Martre, P., 2010. Sowing date and nitrogen fertilisation effects on dry matter and nitrogen dynamics for durum wheat: An experimental and simulation study. Field Crops Res. 117, 245–257. https://doi.org/10.1016/j.fcr.2010.03.010.

Fischer, R.A., 2008. The importance of grain or kernel number in wheat: A reply to Sinclair and Jamieson. Field Crops Res. 105, 15–21. https://doi.org/10.1016/j.fcr.2007.04.002.

Fois, S., Schlichting, L., Marchylo, B., Dexter, J., Motzo, R., Giunta, F., 2011. Environmental conditions affect semolina quality in durum wheat (*Triticum turgidum* ssp. *durum* L.) cultivars with different gluten strength and gluten protein composition. J. Sci. Food Agric. 91, 2664–2673. https://doi.org/10.1002/jsfa.4509.

Fuertes-Mendizábal, T., Aizpurua, A., González-Moro, M.B., Estavillo, J.M., 2010. Improving wheat breadmaking quality by splitting the N fertilizer rate. Eur. J. Agron. 33, 52–61. https://doi.org/10.1016/j.eja.2010.03.001.

Fuertes-Mendizábal, T., González-Torralba, J., Arregui, L.M., González-Murua, C., González-Moro, M.B., Estavillo, J.M., 2013. Ammonium as sole N source improves grain quality in wheat. J. Sci. Food Agric. 93, 2162–2171. https://doi.org/10.1002/jsfa.6022.

Gao, X., Appelbee, M.J., Mekuria, G.T., Chalmers, K.J., Mather, D.E., 2012. A second 'overexpression' allele at the *Glu-B1* high-molecular-weight glutenin locus of wheat: sequence characterisation and functional effects. Theor. Appl. Genet. 124, 333–343. https://doi.org/10.1007/s00122-011-1708-3.

Gao, X., Liu, T., Yu, J., Li, L., Feng, Y., Li, X., 2016. Influence of high-molecular-weight glutenin subunit composition at *Glu-B1* locus on secondary and micro structures of gluten in wheat (*Triticum aestivum* L.). Food Chem. 197, 1184–1190. https://doi.org/10.1016/j.foodchem.2015.11.085.

Gao, X., Tong, J., Guo, L., Yu, L., Li, S., Yang, B., Wang, L., Liu, Y., Li, F., Guo, J., Zhai, S., Liu, C., Rehman, A., Farahnaky, A., Wang, P., Wang, Z., Cao, X., 2020. Influence of gluten and starch granules interactions on dough mixing properties in wheat (*Triticum aestivum* L.). Food Hydrocoll. 106, 105885. https://doi.org/10.1016/j.foodhyd.2020.105885.

Georget, D.M.R., Belton, P.S., 2006. Effects of temperature and water content on the secondary structure of wheat gluten studied by FTIR spectroscopy. Biomacromolecules 7, 469–475. https://doi.org/10.1021/bm050667j.

Goesaert, H., Brijs, K., Veraverbeke, W.S., Courtin, C.M., Gebruers, K., Delcour, J.A., 2005. Wheat flour constituents: how they impact bread quality, and how to impact their functionality. Trends Food Sci. Technol. 16, 12–30. https://doi.org/10.1016/j.tifs.2004.02.011.

Guitman, M.R., Arnozis, P.A., Barneix, A.J., 1991. Effect of source-sink relations and nitrogen nutrition on senescence and N remobilization in the flag leaf of wheat. Physiol. Plant. 82, 278–284. https://doi.org/10.1111/j.1399-3054.1991.tb00094.x.

Guo, L., Wang, Q., Chen, H., Wu, D., Dai, C., Chen, Y., Ma, Y., Wang, Z., Li, H., Cao, X., Gao, X., 2022. Moderate addition of B-type starch granules improves the rheological properties of wheat dough. Food Res. Int. 160, 111748. https://doi.org/10.1016/j.foodres.2022.111748.

Guo, X., Sun, X., Zhang, Y., Wang, R., Yan, X., 2018. Interactions between soy protein hydrolyzates and wheat proteins in noodle making dough. Food Chem. 245, 500–507. https://doi.org/10.1016/j.foodchem.2017.10.126.

Guzmán, C., Autrique, J.E., Mondal, S., Singh, R.P., Govindan, V., Morales-Dorantes, A., Posadas-Romano, G., Crossa, J., Ammar, K., Peña, R.J., 2016. Response to drought and heat stress on wheat quality, with special emphasis on bread-making quality, in durum wheat. Field Crops Res. 186, 157–165. https://doi.org/10.1016/j.fcr.2015.12.002.

Guzmán, C., Crossa, J., Mondal, S., Govindan, V., Huerta, J., Crespo-Herrera, L., Vargas, M., Singh, R.P., Ibba, M.I., 2022. Effects of glutenins (*Glu-1* and *Glu-3*) allelic variation on dough properties and bread-making quality of CIMMYT bread wheat breeding lines. Field Crops Res. 284, 108585. https://doi.org/10.1016/j.fcr.2022.108585.

Ihsan, M.Z., El-Nakhlawy, F.S., Ismail, S.M., Fahad, S., Daur, I., 2016. Wheat phenological development and growth studies as affected by drought and late season high temperature stress under arid environment. Front. Plant Sci. 7, 795. https://doi.org/10.3389/fpls.2016.00795.

Johansson, E., Malik, A.H., Hussain, A., Rasheed, F., Newson, W.R., Plivelic, T., Hedenqvist, M.S., Gällstedt, M., Kuktaite, R., 2013. Wheat gluten polymer structures: the impact of genotype, environment, and processing on their functionality in various applications. Cereal Chem. 90, 367–376. https://doi.org/10.1094/CCHEM-08-12-0105-FI.

Kong, L., Xie, Y., Hu, L., Feng, B., Li, S., 2016. Remobilization of vegetative nitrogen to developing grain in wheat (*Triticum aestivum* L.). Field Crops Res. 196, 134–144. https://doi.org/10.1016/j.fcr.2016.06.015.

Kong, X., Hou, R., Yang, G., Ouyang, Z., 2023. Climate warming extends the effective growth period of winter wheat and increases grain protein content. Agric. For. Meteorol. 336, 109477. https://doi.org/10.1016/j.agrformet.2023.109477.

Labuschagne, M.T., Moloi, J., Van Biljon, A., 2016. Abiotic stress induced changes in protein quality and quantity of two bread wheat cultivars. J. Cereal. Sci. 69, 259–263. https://doi.org/10.1016/j.jcs.2016.03.018.

Laidig, F., Piepho, H.P., Rentel, D., Drobek, T., Meyer, U., Huesken, A., 2017. Breeding progress, environmental variation and correlation of winter wheat yield and quality traits in German official variety trials and on-farm during 1983–2014. Theor. Appl. Genet. 130, 223–245. https://doi.org/10.1007/s00122-016-2810-3.

Li, C., Yang, J., Li, Z., Wang, X., Guo, Z., Tian, Y., Liu, J., Siddique, K.H.M., Wang, Z., Zhang, D., 2023. Integrating crop and soil nutrient management for higher wheat grain yield and protein concentration in dryland areas. Eur. J. Agron. 147, 126827. https://doi.org/10.1016/j.eja.2023.126827.

Li, S., Liu, Y., Tong, J., Yu, L., Ding, M., Zhang, Z., Rehman, A., Majzoobi, M., Wang, Z., Gao, X., 2020a. The overexpression of high-molecular-weight glutenin subunit Bx7 improves the dough rheological properties by altering secondary and microstructures of wheat gluten. Food Res. Int. 130, 108914. https://doi.org/10.1016/j.foodres.2019.108914.

Li, Y., Fu, J., Shen, Q., Yang, D., 2020b. High-molecular-weight glutenin subunits: genetics, structures, and relation to end use qualities. Int. J. Mol. Sci. 22, 184. https://doi.org/10.3390/ijms22010184.

Li, Y., Wu, Y., Hernandez-Espinosa, N., Peña, R.J., 2013. The influence of drought and heat stress on the expression of end-use quality parameters of common wheat. J. Cereal. Sci. 57, 73–78. https://doi.org/10.1016/j.jcs.2012.09.014.

Liu, B., Asseng, S., Liu, L., Tang, L., Cao, W., Zhu, Y., 2016. Testing the responses of four wheat crop models to heat stress at anthesis and grain filling. Glob. Change Biol. 22, 1890–1903. https://doi.org/10.1111/gcb.13212.

Liu, J., 2023. Effects of irrigation and nitrogen fertilizer management on wheat grain baking quality based on the SiriusQuality2 crop model. Irrig. Drain. 72, 729–746. https://doi.org/10.1002/ird.2820.

Liu, J., He, Q., Zhou, G., Song, Y., Guan, Y., Xiao, X., Sun, W., Shi, Y., Zhou, K., Zhou, S., Wu, Y., Ma, S., Wang, R., 2023. Effects of sowing date variation on winter wheat yield: conclusions for suitable sowing dates for high and stable yield. Agronomy 13, 991. https://doi.org/10.3390/agronomy13040991.

Liu, J., Zhang, J., Zhu, G., Zhu, D., Yan, Y., 2022. Effects of water deficit and high N fertilization on wheat storage protein synthesis, gluten secondary structure, and breadmaking quality. Crop J. 10, 216–223. https://doi.org/10.1016/j.cj.2021.04.006.

Lorite, I.J., Castilla, A., Cabezas, J.M., Alza, J., Santos, C., Porras, R., Gabaldón-Leal, C., Muñoz-Marchal, E., Sillero, J.C., 2023. Analyzing the impact of extreme heat events and drought on wheat yield and protein concentration, and adaptation strategies using long-term cultivar trials under semi-arid conditions. Agric. For. Meteorol. 329, 109279. https://doi.org/10.1016/j.agrformet.2022.109279.

Lyu, X., Liu, Y., Li, N., Ku, L., Hou, Y., Wen, X., 2022. Foliar applications of various nitrogen (N) forms to winter wheat affect grain protein accumulation and quality via N metabolism and remobilization. Crop J. 10, 1165–1177. https://doi.org/10.1016/j.cj.2021.10.009.

Ma, S., Wang, T., Guan, X., Zhang, X., 2018. Effect of sowing time and seeding rate on yield components and water use efficiency of winter wheat by regulating the growth redundancy and physiological traits of root and shoot. Field Crops Res. 221, 166–174. https://doi.org/10.1016/j.fcr.2018.02.028.

MacRitchie, F., 2016. Seventy years of research into breadmaking quality. J. Cereal. Sci. 70, 123–131. https://doi.org/10.1016/j.jcs.2016.05.020.

Mahdavi, S., Arzani, A., Mirmohammady Maibody, S.A.M., Kadivar, M., 2022. Grain and flour quality of wheat genotypes grown under heat stress. Saudi J. Biol. Sci. 29, 103417. https://doi.org/10.1016/j.sjbs.2022.103417.

Majláth, I., Darko, E., Palla, B., Nagy, Z., Janda, T., Szalai, G., 2016. Reduced light and moderate water deficiency sustain nitrogen assimilation and sucrose degradation at low temperature in durum wheat. J. Plant Physiol. 191, 149–158. https://doi.org/10.1016/j.jplph.2015.12.004.

Martre, P., Porter, J.R., Jamieson, P.D., Triboï, E., 2003. Modeling grain nitrogen accumulation and protein composition to understand the sink/source regulations of nitrogen remobilization for wheat. Plant Physiol. 133, 1959–1967. https://doi.org/10.1104/pp.103.030585.

Mirosavljević, M., Mikić, S., Župunski, V., Abdelhakim, L., Trkulja, D., Zhou, R., Špika, A. K., Ottosen, C.O., 2024. Effects of heat stress during anthesis and grain filling stages on some physiological and agronomic traits in diverse wheat genotypes. Plants 13, 2083. https://doi.org/10.3390/plants13152083.

Ortolan, F., Urbano, K., Netto, F.M., Steel, C.J., 2022. Chemical and structural characteristics of proteins of non-vital and vital wheat glutens. Food Hydrocoll. 125, 107383. https://doi.org/10.1016/j.foodhyd.2021.107383.

Osman, A.M., Struik, P.C., Lammerts Van Bueren, E.T., 2012. Perspectives to breed for improved baking quality wheat varieties adapted to organic growing conditions. J. Sci. Food Agric. 92, 207–215. https://doi.org/10.1002/jsfa.4710.

Ottaiano, L., Di Mola, I., Cozzolino, E., Mori, M., 2022. Preliminary results of the use of sowing time and variety choice as techniques of adaptability of durum wheat (*Triticum durum* Desf.) to temperature increases. Sustainability 14, 14111. https://doi.org/10.3390/su142114111.

Prystupa, P., Savin, R., Slafer, G.A., 2004. Grain number and its relationship with dry matter, N and P in the spikes at heading in response to N×P fertilization in barley. Field Crops Res. 90, 245–254. https://doi.org/10.1016/j.fcr.2004.03.001.

Rossini, A., Ruggeri, R., Belocchi, A., Rossini, F., 2024. Response of durum wheat cultivars to climate change in a Mediterranean environment: trends of weather and crop variables at the turn of 21st century. J. Agron. Crop Sci. 210, e12786. https://doi.org/10.1111/jac.12786.

Sadras, V.O., Monzon, J.P., 2006. Modelled wheat phenology captures rising temperature trends: shortened time to flowering and maturity in Australia and Argentina. Field Crops Res. 99, 136–146. https://doi.org/10.1016/j.fcr.2006.04.003.

Shah, F., Coulter, J.A., Ye, C., Wu, W., 2020. Yield penalty due to delayed sowing of winter wheat and the mitigatory role of increased seeding rate. Eur. J. Agron. 119, 126120. https://doi.org/10.1016/j.eja.2020.126120.

Shewry, P.R., Halford, N.G., Tatham, A.S., 1992. High molecular weight subunits of wheat glutenin. J. Cereal. Sci. 15, 105–120. https://doi.org/10.1016/S0733-5210(09)80062-3.

Siddique, K.H.M., Kirby, E.J.M., Perry, M.W., 1989. Ear: Stem ratio in old and modern wheat varieties; relationship with improvement in number of grains per ear and yield. Field Crops Res. 21, 59–78. https://doi.org/10.1016/0378-4290(89)90041-5.

Singh, H., MacRitchie, F., 2001. Application of polymer science to properties of gluten. J. Cereal. Sci. 33, 231–243. https://doi.org/10.1006/jcrs.2000.0360.

Singh, N., Virdi, A.S., Katyal, M., Kaur, A., Kaur, D., Ahlawat, A.K., Singh, A.M., Kumar Sharma, R., 2021. Evaluation of heat stress through delayed sowing on physicochemical and functional characteristics of grains, whole meals and flours of India wheat. Food Chem. 344, 128725. https://doi.org/10.1016/j.foodchem.2020.128725.

Sissons, M., Pleming, D., Taylor, J.D., Emebiri, L., Collins, N.C., 2018. Effects of heat exposure from late sowing on the agronomic and technological quality of tetraploid wheat. Cereal Chem. 95, 274–287. https://doi.org/10.1002/cche.10027.

Slafer, G.A., Savin, R., 1994. Source–sink relationships and grain mass at different positions within the spike in wheat. Field Crops Res. 37, 39–49. https://doi.org/10.1016/0378-4290(94)90080-9.

Sun, H., Zhang, X., Chen, S., Pei, D., Liu, C., 2007. Effects of harvest and sowing time on the performance of the rotation of winter wheat–summer maize in the North China Plain. Ind. Crop. Prod. 25, 239–247. https://doi.org/10.1016/j.indcrop.2006.12.003.

Tao, Z., Chang, X., Wang, D., Wang, Y., Ma, S., Yang, Y., Zhao, G., 2018. Effects of sulfur fertilization and short-term high temperature on wheat grain production and wheat flour proteins. Crop J. 6, 413–425. https://doi.org/10.1016/j.cj.2018.01.007.

Toyota, M., Morokuma, M., 2021. Morphological and phenological adaptation for convergent development of tillers in widely spaced wheat sown on different dates. Plant. Prod. Sci. 24, 52–64. https://doi.org/10.1080/1343943X.2020.1808485.

Triboi, E., 2003. Environmentally induced changes in protein composition in developing grains of wheat are related to changes in total protein content. J. Exp. Bot. 54, 1731–1742. https://doi.org/10.1093/jxb/erg183.

Urade, R., Sato, N., Sugiyama, M., 2018. Gliadins from wheat grain: an overview, from primary structure to nanostructures of aggregates. Biophys. Rev. 10, 435–443. https://doi.org/10.1007/s12551-017-0367-2.

Visioli, G., Bonas, U., Dal Cortivo, C., Pasini, G., Marmiroli, N., Mosca, G., Vamerali, T., 2018. Variations in yield and gluten proteins in durum wheat varieties under late-season foliar *versus* soil application of nitrogen fertilizer in a northern Mediterranean environment. J. Sci. Food Agric. 98, 2360–2369. https://doi.org/10.1002/jsfa.8727.

Wang, H., Zhong, L., Fu, X., Huang, S., Zhao, D., He, H., Chen, X., 2023a. Physiological analysis reveals the mechanism of accelerated growth recovery for rice seedlings by nitrogen application after low temperature stress. Front. Plant Sci. 14, 1133592. https://doi.org/10.3389/fpls.2023.1133592.

Wang, S., Niu, Y., Shang, L., Li, Z., Lin, X., Wang, D., 2023b. Supplemental irrigation at the jointing stage of late sown winter wheat for increased production and water use efficiency. Field Crops Res. 302, 109069. https://doi.org/10.1016/j.fcr.2023.109069.

Wijerathna-Yapa, A., Pathirana, R., 2022. Sustainable agro-food systems for addressing climate change and food security. Agriculture 12, 1554. https://doi.org/10.3390/agriculture12101554.

Yang, L., Guo, S., Chen, Q., Chen, F., Yuan, L., Mi, G., 2016. Use of the stable nitrogen isotope to reveal the source-sink regulation of nitrogen uptake and remobilization during grain filling phase in maize. PLoS One 11, e0162201. https://doi.org/10.1371/journal.pone.0162201.

Yao, B., Ata-Ul-Karim, S.T., Li, Y., Ye, T., Zhu, Y., Cao, W., Cao, Q., Tang, L., 2023. Plant nitrogen status at phenological stages can well estimate wheat yield and its components. Field Crops Res. 297, 108950. https://doi.org/10.1016/j.fcr.2023.108950.

Yu, L., Ma, Y., Zhao, Y., Rehman, A., Guo, L., Liu, Y., Yang, Y., Wang, Z., Cao, X., Gao, X., 2022. Interaction of B-type starch with gluten skeleton improves wheat dough mixing properties by stabilizing gluten micro-structure. Food Chem. 371, 131390. https://doi.org/10.1016/j.foodchem.2021.131390.

Zhang, G., Liu, S., Dong, Y., Liao, Y., Han, J., 2022a. A nitrogen fertilizer strategy for simultaneously increasing wheat grain yield and protein content: mixed application of controlled-release urea and normal urea. Field Crops Res. 277, 108405. https://doi.org/10.1016/j.fcr.2021.108405.

Zhang, X., Chen, S., Sun, H., Wang, Y., Shao, L., 2010. Water use efficiency and associated traits in winter wheat cultivars in the North China Plain. Agric. Water Manage. 97, 1117–1125. https://doi.org/10.1016/j.agwat.2009.06.003.

Zhang, Y., Zhang, Y., Liu, N., Su, D., Xue, Q., Stewart, B.A., Wang, Z., 2012. Effect of source–sink manipulation on accumulation of micronutrients and protein in wheat grains. J. Plant Nutr. Soil Sci. 175, 622–629. https://doi.org/10.1002/jpln.201100224.

Zhang, Z., Xing, Z., Zhou, N., Zhao, C., Liu, B., Jia, D., Wei, H., Guo, B., Zhang, H., 2022b. Effects of post-anthesis temperature and radiation on grain filling and protein quality of wheat (*Triticum aestivum* L.). Agronomy 12, 2617. https://doi.org/10.3390/agronomy12112617.

Zheng, B., Chenu, K., Fernanda Dreccer, M., Chapman, S.C., 2012. Breeding for the future: what are the potential impacts of future frost and heat events on sowing and flowering time requirements for Australian bread wheat (*Triticum aestivium*) varieties? Glob. Change Biol. 18, 2899–2914. https://doi.org/10.1111/j.1365-2486.2012.02724.x.

Zheng, B., Zhang, X., Wang, Q., Li, W., Huang, M., Zhou, Q., Cai, J., Wang, X., Cao, W., Dai, T., Jiang, D., 2021. Increasing plant density improves grain yield, protein quality and nitrogen agronomic efficiency of soft wheat cultivars with reduced nitrogen rate. Field Crops Res. 267, 108145. https://doi.org/10.1016/j.fcr.2021.108145.

Zhong, Y., Yang, M., Cai, J., Wang, X., Zhou, Q., Cao, W., Dai, T., Jiang, D., 2018. Nitrogen topdressing timing influences the spatial distribution patterns of protein components and quality traits of flours from different pearling fractions of wheat (*Triticum aestivum* L.) grains. Field Crops Res. 216, 120–128. https://doi.org/10.1016/j.fcr.2017.11.016.

Zhu, Y., Chu, J., Dai, X., He, M., 2019. Delayed sowing increases grain number by enhancing spike competition capacity for assimilates in winter wheat. Eur. J. Agron. 104, 49–62. https://doi.org/10.1016/j.eja.2019.01.006.

Zhu, Y., Liu, J., Li, J., Xian, L., Chu, J., Liu, H., Song, J., Sun, Y., Dai, Z., 2023. Delayed sowing increased dry matter accumulation during stem elongation in winter wheat by improving photosynthetic yield and nitrogen accumulation. Eur. J. Agron. 151, 127004. https://doi.org/10.1016/j.eja.2023.127004.